NUMERICAL STUDY OF CONVECTIVE HEAT TRANSFER FOR A TURBULENT FLOW IN A CORRUGATED TUBE USING NANOFLUID

MD. MAHBUBUR RAHMAN

Department of Mechanical Engineering
Military Institute of Science and Technology (MIST)
Dhaka, Bangladesh

January 2019

NUMERICAL STUDY OF CONVECTIVE HEAT TRANSFER FOR A TURBULENT FLOW IN A CORRUGATED TUBE USING NANOFLUID

A Thesis Submitted to the Department of Mechanical Engineering, Military Institute of Science and Technology in Partial Fulfillment of the Requirements for the Degree of Masters of Science in Mechanical Engineering

MD. MAHBUBUR RAHMAN

(*MSc Engg., MIST*)

Department of Mechanical Engineering
Military Institute of Science and Technology (MIST)
Dhaka, Bangladesh

January 2019

The thesis titled **"NUMERICAL STUDY OF CONVECTIVE HEAT TRANSFER FOR A TURBULENT FLOW IN A CORRUGATED TUBE USING NANOFLUID"** Submitted by **Md. Mahbubur Rahman** Roll No: **1014180007 (P)** Session: 2014-15 has been accepted as satisfactory in partial fulfillment of the requirement for the degree of Master of Science in Mechanical Engineering on ……. January 2019.

BOARD OF EXAMINERS

…… Professor Dr. A. K. M. Sadrul Islam Ex-Head, Department of Mechanical Engineering BUET, Dhaka-1000, Bangladesh	**Chairman (Supervisor)**
…… Col Md Humayun Kabir Bhuiyan, psc Head, Department of Mechanical Engineering, MIST Dhaka-1216, Bangladesh	**Member (Ex-Officio)**
…… Professor Dr. Md. Quamrul Islam Department of Mechanical Engineering, MIST Dhaka-1216, Bangladesh	**Member (Internal)**
…… Brig Gen Md Lutfor Rahman, PhD Vice Chancellor, BAUST, Saidpur.	**Member (External)**
…… Professor Dr. Mohammad Ali Department of Mechanical Engineering, BUET Dhaka-1000, Bangladesh	**Member (External)**

DECLARATION

I with this declare that this thesis is my original work and I have written it in its entirety. I have duly acknowledged all the sources of information which have been used in the thesis. This thesis has also not been submitted for any degree in any university previously.

…….

Md. Mahbubur Rahman

January 2019

DEDICATED

TO

MY PARENTS AND WIFE

ACKNOWLEDGEMENT

At the very outset, the author expresses his deepest gratitude and profound indebtedness to his supervisor, Dr. A. K. M. Sadrul Islam, Professor, Ex-Head, Department of Mechanical Engineering, BUET, Dhaka for his continuous guidance, valuable suggestions and encouragement throughout the research work. His real help and valuable advice at every stage made this research work possible.

The author is thankful to Capt (Retd) Anwarul Haque Chowdhury, BN for his continuous support and encouragement. The support provided by the Head of the Department, Department of Mechanical Engineering is also duly acknowledged.

Finally, I would like to express my sincere thanks to all members of the Department of Mechanical Engineering of MIST for their cooperation and help in the successful completion of the work.

ABSTRACT

Heat transfer enhancement can be done in different ways, but the use of nanofluid is one of the latest approaches. A numerical investigation of turbulent forced convection through a right-angled triangular-shaped corrugated tube is presented by using commercial computational fluid dynamics software, ANSYS Fluent. The length and diameter of the tube which is considered for the study are 200 mm and 8 mm respectively and a uniform constant heat flux of 5,000 W/m^2 is applied at the corrugated wall boundary. A 2D simulation with the axisymmetric model is considered for analyzing different parameters. The corrugation has an amplitude of 1.60 mm and a wavelength of 6 mm. Realizable k-ε turbulent model is employed with enhanced wall treatment for the analysis. Nanofluid is allowed to flow with uniform velocity and uniform temperature of 300 K at the inlet of the pipe with an assumption of a no-slip condition. Heat transfer parameter like convective heat transfer coefficient and fluid dynamics parameter like friction factor and pumping power are calculated using three different nanofluids, namely Al_2O_3-water, TiO_2-water, and CuO-water of different volume fraction (1%, 2%, 3%, 4% and 5%) for a range of Reynolds number 5000 to 25000. The result shows that the heat transfer coefficient increases with the increase in volume fraction of the nanofluid as well as with the Reynolds number. That is 44.66% for Al_2O_3-water, 27.35% for TiO_2-water and 25.74% CuO-water nanofluid at Reynolds number of 25000 and 5% volume fraction.

CONTENTS

LIST OF TABLES

LIST OF FIGURES

NOMENCLATURE

A_c	Cross-sectional area of circular tube
A_w	Surface area of circular tube
C_p	Specific heat at constant pressure
D_h	Hydraulic diameter
d_p	Particle diameter
f	Friction factor
h_c	Average heat transfer coefficient
k	Thermal conductivity
M	Molecular weight of the base fluid molecule
$\dot{m}$	Mass flow rate
$\dot{V}$	Volumetric flow rate
W	Pumping power per unit length of the pipe
ΔP	Differential pressure loss
N	Avogadro number
Q	Heat transfer
t	Tube wall thickness
T	Temperature
T_o	Reference temperature, 273 K
U	Velocity of flow at inlet
K_B	Boltzmann's constant

Greek symbols

ϕ	Volume fraction
μ	Dynamic viscosity
ν	Kinematic viscosity
ρ	Mass density

Subscripts

av	Average value
i	Inlet Value
o	Outlet Value
nf	Nanofluid
bf	Basefluid
np	Nanoparticle
w	wall

Dimensionless parameter

N_u	Nusselt number
R_e	Reynolds number
P_r	Prandl number

CHAPTER ONE

INTRODUCTION

1.1 Background of the Study

Now a day's heat transfer is one of the fundamental and burning issues of thermal engineering which influences our everyday life significantly. A sufficient amount of heat removal or addition moving from one process stream to another is one of the significant challenges in numerous industries, including power generation, transportation, manufacturing, air conditioning, cooling, heating, lubricating, etc. Apart from conduction energy is carried out with the fluid in automobiles, refrigerators, heat exchangers, air-condition system, cooling, and lubricating system, etc. The fluid carries system's energy. On the other hand, fluid is the main phenomena to control the behavior of heat transfer. To improve heat transfer efficiency and to reduce pumping power, pressure loss, frictional loss between any physical systems several methods have been developed in the last few decades

Among these methods, some are the utilization of the extended surface of the physical system, application of vibration to the heat transfer surface, use of microchannels, utilization of fins, etc. Heat transfer can also be improved by increasing the thermal conductivity of the working fluid. At present maximum researchers give more concentration on improving the thermal conductivity of working fluids. Where water, ethylene glycol, and engine oil are commonly used as heat transfer fluid. However, this fluid has relatively low thermal conductivity compared to the thermal conductivity of solids. By adding a small number of old particles with the base or working fluid, the thermal conductivity of the fluid can be increased noticeably. Thus the ability of the utilization of engineered colloidal suspension of solids particles with sizes on order 2 millimeters or micrometers was previously investigated by several researchers and following significant drawbacks were obtained by Choi et al. [1].

- The particle which forms a layer on the surface and reducing the heat transfer capacity on the fluid.
- If the circulation rate of the fluid is increased then the sedimentation is reduced but the erosion of the heat transfer devices, pipelines, etc. increasing rapidly.

- The large size of the particles tends to clog the flow channels, mainly if the cooling channels are narrow.
- The pressure drop in the fluid decrease rapidly.
- Finally, conductivity enhancement based on practice concentration is achieved, i.e. the highest particle volume fraction is the higher the enhancement and higher the problems as indicated above.

Based on the above statement it is found that the utilization of small particles in the liquid was introduced but not accepted option for heat transfer application. However, this investigation provided and opened a new area for researchers which quite different from the parent material in mechanical, thermal, electrical and optical properties.

However, the situation has changed when Choi et al. [2] reinvestigated with their Nanoscale metallic particle and carbon nanotube suspensions in Argonne National Laboratory. Choi et al. [3] and Zhang et al. [4] have tried to suspend various metal and metal oxides nanoparticles in several different fluids, and their result is promising. From their investigation, they also observed that many things remain vacuous about these suspensions of Nano-structured materials, Choi and Eastman have been termed these as “Nanofluid.”

The use of nanoparticles in a base fluid results in significant improvement in thermo-physical properties of the mixer fluid like thermal conductivity, viscosity, electrical conductivity, Seebeck coefficient, and optical scattering coefficient, etc. which contribute to the enhancement of heat transfer rate. Carbon nanotubes are commonly used Nanoproperties which are used in nanofluids. Nanoparticles or fluids are produced in several techniques. They are:

- Direct evaporation (1 step).
- Gas condensation (2 steps).
- Chemical vapor condensation (1step).
- Chemical precipitation (1step).

The reasons behind the enhancement of thermal properties by addition of nanoparticle are as follows By Xuan et al. [5]:

- The suspended nanoparticles are increasing the relative surface area of the fluid.

- The suspended nanoparticles are increasing the effective thermal conductivity of the fluid.
- The mixing fluctuation and turbulence of the fluid are intensified.
- The dispersion of nanoparticles flattens transverse temperature gradient of fluid.

Various factors like particle shape and size, density, viscosity, percentage, clustering of particles, the temperature of fluid and dissociation of surfactant, etc. also affect the thermal properties of nanofluids. The first test with nanofluid that was done by Choi and Das providing many encouraging features. The four unique features observed are listed below Choi et al. [1]:

- **Abnormal enhancement of thermal conductivity:** Abnormal rise in thermal conductivity was the most essential feature in nanofluid which was much far beyond expectation and much higher than any other theory could predict.
- **Stability:** Using stability agent it could be stable over months.
- **Small concentration and Newtonian behavior:** By using a small concentration of nanofluid about 1% to 5% substantial enhancement of thermal conductivity was achieved, and it entirely maintained the Newtonian behavior of the fluid. The rise in viscosity was nominal, and the pressure drop was increased only marginally.
- **Particle size dependence:** Size of Nano-particles also affects the thermal conductivity. In general, with decreasing particle size an increase in enhancement was observed.

1.2 Nanoparticle and Base Fluid

Most of the researchers frequently use Al_2O_3, CuO, Ti_2O, SiC, TiC, ZnO, Fe_2O_3, Ag, Au, Cu, and Fe nanoparticle frequently a minimal amount for preparing nanofluid. These nanoparticles are used because of their high thermal conductivity and high heat transfer capacity. The performance and selection of nanoparticle depend on the two factors:

a. Particle size
b. Particle shape

1.2.1 Particle size

The particle size of nanoparticles should be less than 100nm to get more heat transfer. Researchers usually use 10nm to 100nm particle size for their investigation. Even the

particles size should not exceed 100nm when the rod or tube-shaped materials are used instead of spherical particles, but in this case, the length of the particles may be on the order of micrometers. One another vital behavior of nanoparticles is clustering phenomena by which particles may form clusters with sizes on the order of micrometer.

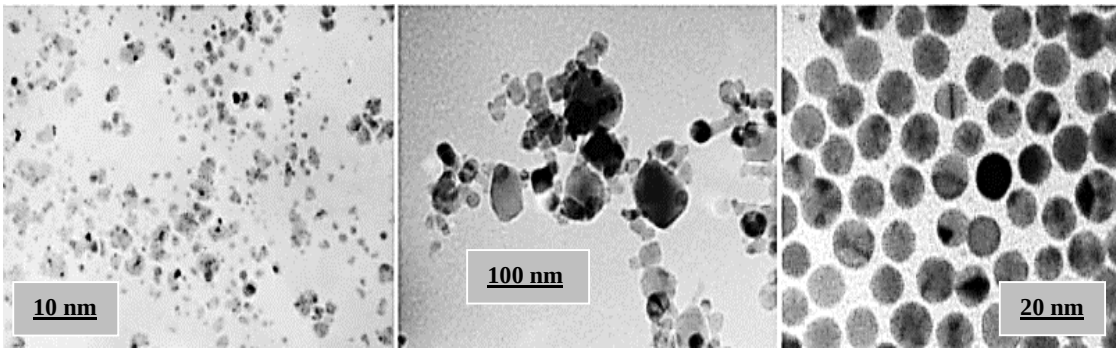

Figure 1.1 Different types of Particle Size of Al_2O_3 nanoparticles by Piccolo et al. [6]

1.2.2 Particles shape

Usually, different types of shapes are used of nanoparticles among them most of the researchers use spherical shaped for their investigation. Other types of shaped like rod-shaped, tube-shaped and disk-shaped are also used. Besides this, the clusters formed by nanoparticle may have fractal-like shapes.

Base fluid indicates the primary working fluid of heat transfer application for preparing nanofluid. Mainly water, ethylene glycol, and engine oil are used as base fluid through the whole world. Usually, the small size of nanoparticles is mixed with base fluid to prepare the nanofluid. So the base fluid's properties like thermal conductivity, density, viscosity, specific heat, etc. are affected and controlled by volume fraction, shape and size of the nanoparticles.

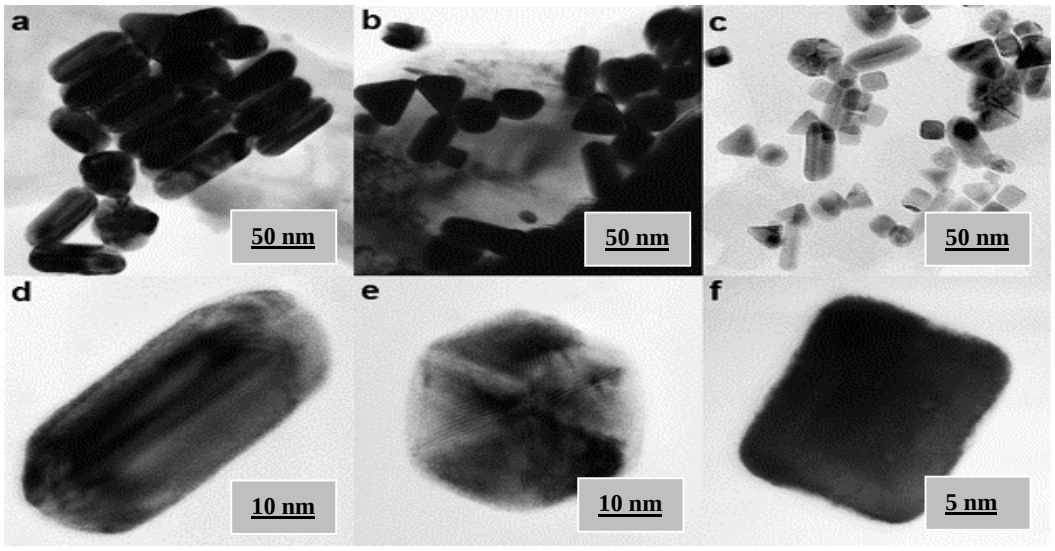

Figure 1.2 Different types of particle shape of Al_2O_3 nanoparticles Philip et al. [7]

1.3 Preparation Method of Nanofluids

The crucial first step in experimental studies with nanofluids is the preparation of nanofluids. There two well-known and most popular methods are available throughout the world they are:

a. One or Single Step Method
b. Two Step Method

1.3.1 One or single step method

Single step method is the process which simultaneously produces and disperses the nanoparticles directly into a single step in the base fluid medium that is suitable for metallic nanofluid. Initially, gas phase nanoparticles are solidified in this method. This method is mainly divided into two categories:

a. Direct evaporation-condensation method.
b. Inert gas technique.

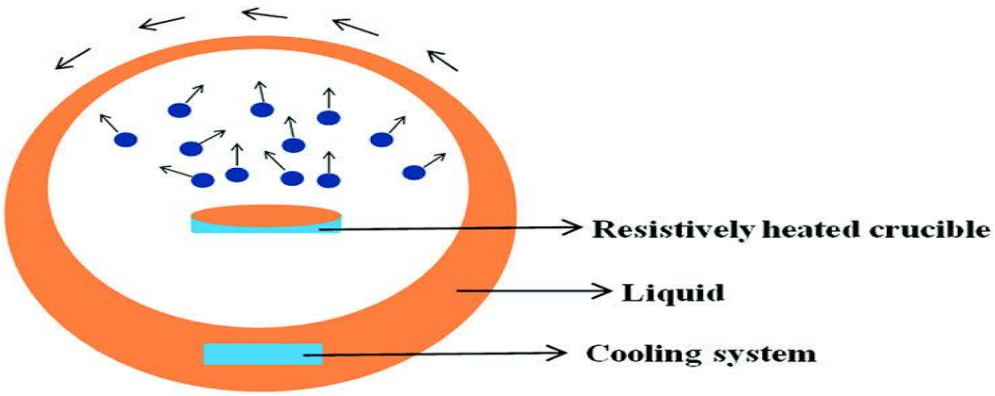

Figure 1.3 One-step synthesis process of nanofluids Jianlin et al. [8]

1.3.2 Two-step method

The two-step method is the most economical and common method than single step which is shown figure 1.4. In this process, at first the Nano sized solid particles such as Nanorods, nanotubes, Nanofibers or other functionalized nanomaterials are synthesized in powder form by the chemical or physical process and then these powder particles are dispersed in the base fluid which is down by two way Mukherjee et al. [9]:

a. Intensive ultra-sonication method
b. Using surfactants

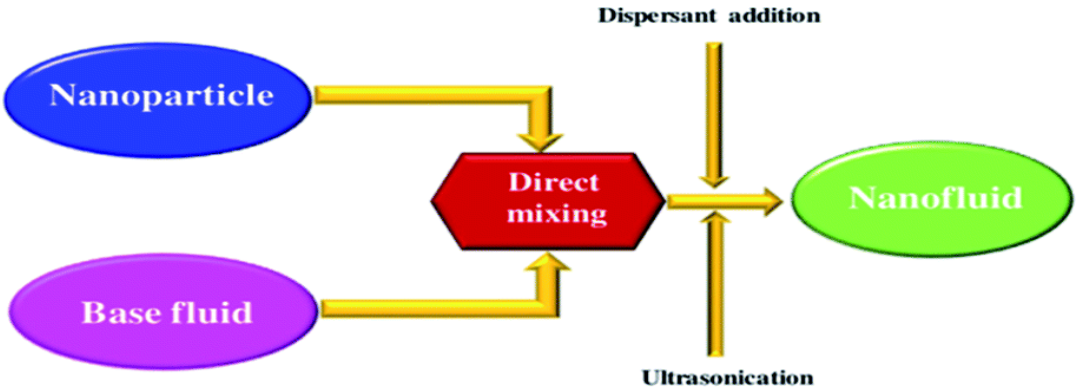

Figure 1.4 Two-step synthesis process of preparing nanofluids by Jianlin et al. [8]

Table 1.1 Researches on synthesis process Jianlin et al. [8]:

Author	Nanofluids	Synthesis process
Patel et al.	Au/Toluene	Two-step
Patel et al.	Ag/Toluene	Two-step
Xie et al.	Al_2O_3/EG	Two-step
Liu at al.	Cu/H_2O	Single-step
Eastman and Choi	Cu/EG	Single-step
Hong et al.	Fe/EG	Single-step
Putnam t al.	Au/Ethanol	Two-step
Xie et al.	CNTs/Decene	Two-step
Xie et al.	CNTs/EG	Two-step
Xie et al.	CNTs/ H_2O	Two-step
Choi et al.	CNTs/Poly oil	Two-step
Liu at al.	CNTs/Engine oil	Two-step
Zhu et al.	Fe_3O_4/ H_2O	Single-step
Xie et al.	SiC/ H_2O	Two-step
Murshed et al.Xie et al.	TiO_2/ H_2O	Two-step
Xie et al.	Al_2O_3/ H_2O	Two-step
Zhang et al.	CuO/ H_2O	Two-step
Xuan and Li	Cu/ H_2O	Two-step
Yang et al.	H_2O/FC-72	Two-step

1.3.3 Other method

There are some other methods which also used for making different types of nanofluid they are Mukherjee et al. [9]:

a. Organic Phase Method
b. Phase Transfer Method
c. Novel Precursor Transformation Method

1.4 Nanoparticle and Base Fluid

Nanofluid is used extensively in heat transfer application such as industrial cooling, smart fluids, cooling of the microchip, sensing and imaging, antibacterial activity, Nano drug delivery, etc. In mechanical application, nanofluid is used in friction reduction and magnetic sealing. In present situation two historic development that stands rightly at the crosshead as it signifies heat transfer technology, i.e. miniaturization on one side and an even astronomical rise at the other. Because of vividly different properties nanofluid is also utilized in advanced heat transfer fluids about two decades now but most potential benefits are using these fluids for concerned heat transfer application. Nanofluid is used for cooling automobile engine and welding equipment. These fluids are also used to cool high heat flux devices such as a high power microwaves tubes and a high power laser diode. To improve the efficiency of MEMS, a nanofluid coolant passes through a tiny passage. In the microprocessor, micro electro mechanical system and in the fluid of biotechnology nanofluid is widely used. In biomedical and Nanomedicine applications such as Nano drug delivery, cancer therapeutics, and sensing and imaging and Nano-cryosurgery nanofluids have been used. Magnetic nanofluids such as hyperthermia, magnetic cell separations and contrast improvement in magnetic resonance imaging. Nanofluid is also applied in enhanced oil recovery (EOR) process, anticorrosive coatings, wet ability alteration, environmental remediation, inkjet printing, etc.

Figure 1.5 Application of nanofluids in heat transfer

1.5 Nanofluid Thermal Application

Cooling is one of the essential scientific challenges in different industries. Therefore, among all applications of NFs, their potential for heat transfer applications have attracted the most attention of Eastman et al. [10]. In metal cutting metal processing data centers and electronic cooling system, it is used.

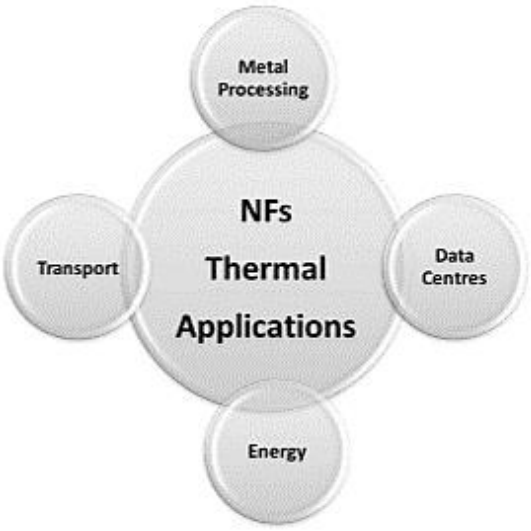

Figure 1.6 Thermal application of nanofluids

For mass transfer enhancement of nanofluid several types of research have been studied. Kim et al. [11] initially examined the effect of nanoparticles on the bubble type absorption for NH_3/H_2O absorption system. The absorption performance enhances up to 3.21 times. Then they visualized the bubble behavior during the NH_3/H_2O absorption process and studied the effect of nanoparticles and surfactants on the absorption

characteristics. Which increases the performance up to 5.32 times. During the ammonia bubble absorption process the addition of both surfactants and nanoparticles enhanced the absorption performance significantly. Some are given in details below:

1.5.1 Industrial cooling applications

The nanofluid application is greatly applied in industrial cooling for energy saving and reduction of emissions. The specific heat of nanofluids was found to be 50% higher for nanofluids compared with poly alpha olefin, and it increased with temperature, and thermal diffusivity is 4 times higher for nanofluid. The liquid metal with a low melting point is expected to be an idealistic base fluid for making a superconductive solution which may lead to the ultimate coolant in a wide variety of heat transfer enhancement area.

1.5.2 Energy applications

Two remarkable properties of nanofluids are utilized for energy applications of nanofluids. One is higher thermal conductivities of nanofluids, enhancing the heat transfer, and another is the absorption properties of nanofluids. The storage of thermal energy in the form of sensible and latent heat has become an essential aspect of energy management with the emphasis on efficient use and conservation of the waste heat and solar energy in industry and buildings by Demirbas [12]. Supercooling degree of water is decreased remarkably by addition Al_2O_3 nanoparticles. It is showed on the thermal response test**.**

1.5.3 Mechanical applications

Nanofluids exhibit excellent lubricating properties because the main reason is that Nanoparticles in nanofluids form a protective film with low hardness and elastic modulus on the work surface. Magnetic fluids are kinds of special nanofluids that have extremely low leakage in an extensive range of applications, and it utilizes magnetic nanoparticles property in liquid.

- **Friction reduction**

Due to load-carrying capacity, good extreme pressure and friction reducing properties nanoparticles have attracted much interest in recent years. Nanofluid’s advanced lubricant can develop productivity through energy protection and energy reliability. Friction and wear are reduced by Tribological research which is heavily emphasized. The tribological behavior of Cu nanoparticles in oil on a four-ball machine. The results

showed that Cu nanoparticles as an oil additive had better friction-reduction and anti-wear properties than zinc dithiophosphate, especially at high applied load. Meanwhile, the nanoparticles could also strikingly improve the load-carrying capacity of the base oil. The smearing of solid particles was found to play a vital role, mainly when a slurry layer was formed. In the minimum quantity lubrication (MQL) grinding process of cast iron water-based Al_2O_3 and nanofluids were used.

- **Magnetic sealing**

Magnetic fluids (Ferromagnetic fluid) are static colloidal suspensions of little magnetic particles such as magnetite (Fe_3O_4). By Kalpana et al. [13] the magnetic component of magnetic nanofluids may be tailored by varying their size and adapting their surface coating to meet the requirements of colloidal stability of magnetic nanofluids with non-polar and polar carrier liquids. Ferro cobalt magnetic fluid was used for oil sealing, and the holding pressure is 25 times as high as that of conventional magnetite sealing it is observed by Pramod et al. [14].

1.5.4 Biomedical application

Nanofluids containing antibacterial activities or drug delivery properties for particular kind of Nanoparticles and exhibit some relevant properties.

- Antibacterial activity
- Nano drug delivery

Space and defense: Due to the restriction of space, energy, and weight in space station and aircraft, there is a strong demand for the highly efficient cooling system with a smaller size. Vassallo et al. [15] have reported the order of magnitude increases in the critical heat flux in pool boiling with nanofluids compared to the base fluid alone. Further research of nanofluids leads to the development of next generation of cooling devices that incorporate nanofluid for ultrahigh-heat-flux electronic systems, presenting the possibility of raising chip power in electronic components or simplifying cooling requirements for space applications. Many military devices and systems require high-heat flux cooling to the level of tens of MW/m2. At this level, the cooling of military devices and system is vital for the reliable operation. Nanofluids with high critical heat fluxes have the potential to provide the required cooling in such applications as well as in other military systems, including military vehicles, submarines, and high-power laser

diodes. Therefore, nanofluids have broad application in space, and defense fields where power density is very high and the components should be smaller and weightless.

Atomic Systems Cooling: The Massachusetts Institute of Technology has set up an interdisciplinary place for Nanofluid innovation for the atomic vitality industry. The specialists Vassallo et al. [15] are investigating the atomic uses of Nanofluids, specifically the accompanying three: (1) primary power source coolant for pressurized water reactors (PWRs). It could empower significant control up rates in the present and future PWRs, in this manner improving their financial execution. Specifically, the utilization of Nanofluids with no less than 32% higher basic warmth flux (CHF) could empower a 20% power thickness uprate in momentum plants without changing the fuel get together to outline and without lessening the edge to CHF; (2) coolant for the crisis center cooling frameworks (ECCSs) of the two PWRs and bubbling water reactors. The utilization of a Nanofluid in the ECCS aggregators and wellbeing infusion can expand the pinnacle cladding-temperature edges (in the ostensible power center) or keep up them in uprated centers if the Nanofluid has a higher post-CHF warm exchange rate; (3) coolant for in vessel maintenance of the liquid center amid serious mishaps in high-control thickness light water reactors. It can build the edge to vessel break by 40% amid extreme mishaps in high-control thickness frameworks, for example, Westinghouse APR1000 and the Korean APR1400. While there exist a few significant holes, including the nanofluid warm water, had driven execution at prototypical reactor conditions and the similarity of the nanofluid science with the reactor materials. Much work ought to be done to overcome these gaps before any applications can implement nuclear control plant.

Nanofluids as Vehicular Brake Fluids: A vehicle's kinetic vitality is scattered through the warmth delivered amid the way toward breaking and this is transmitted all through the brake fluid in the pressure-driven stopping mechanism. Copper-oxide and aluminum-oxide based brake nanofluids were made utilizing the curve submerged nanoparticle blend framework and the plasma charging circular segment framework, separately. The two sorts of nanofluids both have improved properties, for example, a higher breaking point, higher consistency, and a higher conductivity than that of customary brake fluid. By yielding a higher breaking point, conductivity, and thickness, the nanofluid brake oil decrease the event of vapor-bolt and offer expanded security while driving.

Nanofluids-Based Microbial Fuel Cell: Microbial power devices (MFC) that use the vitality found in sugars, proteins, and other vitality rich regular items to create electrical influence have a promising future. The astounding execution of MFC relies upon anodes and electron. Sharma et al. [16] built a new microbial power module (MFC) utilizing a novel electron go-between and CNT based anodes. The novel middle people are nanofluids which were set up by scattering Nanocrystalline platinum moored CNTs in water. They analyzed the execution of the new E. coli-based MFC to the beforehand specific E. coli-based microbial power devices with impartial red and methylene blue electron arbiters. The execution of the MFC utilizing CNT-based nanofluids and CNT-based anodes has been thought about against plain graphite electrode based MFC. CNT-based anodes appeared as high as fold increment in the power thickness contrasted with graphite terminals. The work shows the capability of respectable metal nanoparticles scattered on CNT-based MFC for the age of high energies from even primary microscopic organisms like E. coli.

1.5.5 Others application

a. Cancer Therapeutics.
b. Nano cryosurgery.
c. Sensing and imaging.
d. Cryopreservation nanofluid detergent.
e. Intensify microreactors,
f. Nanofluids as vehicular brake fluids,
g. Nanofluids based microbial fuel cell,
h. Nanofluids as optical filters.

1.6 Objectives of the Thesis

The research work is based on enhancement of convective heat transfer coefficient using nanofluid with different shape of channels. However, the information regarding the requirement of pumping power is decidedly less which will be taken into consideration. The objectives of the project are as follows:

a. To measure the convective heat transfer coefficient using different nanofluid (CuO, Al_2O_3 and TiO_2) in a right-angled triangular-shaped corrugated tube for turbulent flow (Reynolds number 5000 to 25000) using ANSYS Fluent.
b. To determine the convective heat transfer coefficient using different volume fraction of nanofluid.
c. To measure optimum requirement of pumping power.

The result enables the engineers to design heat exchanger equipment efficiently. Since the results will be expressed in the non-dimensional form, they may be applied for a prototype application.

CHAPTER TWO

LITERATURE REVIEW

2.1 Research on Nanofluid

Heat transfer equipment is extensively used in all aspects of engineering applications, such as HVAC systems, refrigeration systems, automobile radiators, electronic devices, process industries, etc. Numerous scientific researches have been carried out in the past few decades to discover a suitable heat transfer fluid to design more compact heat exchanger with excellent thermal efficiency. Nanotechnology offers a novel approach in intensifying the heat transfer characteristics by utilizing the higher thermal conductivity of solid nanoparticles. In recent years heat transfer augmentation achieved tremendous momentum due to the increased demand for energy consumption optimization in a great deal of industrial and engineering equipment, such as compact heat exchangers.

Behzadmehr et al. [17] worked with Cu-water nanofluid to investigate the turbulent convective heat transfer characteristics in a circular tube by a single-phase model and results were compared with a mixture model. A significant enhancement of average Nusselt number was observed with Reynolds number increment.

Santra et al. [18] studied the heat transfer numerically with Cu-water nanofluid under laminar flow conditions through two isothermally heated parallel plates considering nanofluid as a cooling medium. The heat transfer rate was enhanced with an increase of Reynolds number and particle volume concentration.

Heidary and Kermani [19] presented a numerical work to investigate the effect of Reynolds number, particle volume fraction, and wave amplitude on Nusselt number and skin friction coefficient in the sinusoidal-wall channel for constant wall temperature. Cu-water was used as the nanofluid and, a maximum 50% enhancement of heat transfer was found as compared to water. Ahmed et al. [20] reported a considerable enhancement of heat transfer by employing nanofluid through an isothermally heated triangular-shaped corrugated channel for a range of Reynolds number 100-1000 and nanoparticle volume fraction up to 5%.

Vatani and Mohammed [21] studied turbulent convective heat transfer to observe the thermal and hydraulic performance in rectangular, triangular, and arc-shaped rib-grooved channels and a comparison was made between Al_2O_3, SiO_2, CuO, ZnO nanoparticles using water as the base fluid. SiO_2-water nanofluid provided the highest average Nusselt number while rectangular-shaped rib-grooved channel showed better performance concerning performance evaluation criterion.

Talebi et al. [22] provided a numerical study of mixed convection flow in a square lid-driven cavity for a range of Rayleigh number 10^4-10^6, Reynolds number 1-100 and volume fraction up to 0.05%. The results revealed that at relatively higher Rayleigh number, the volume fraction of nanoparticles had a profound effect on the flow pattern and thermal performance.

Abu-Nada et al. [23] showed the natural convection heat transfer intensification in horizontal concentric annuli using four different types of water-based nanofluids. Among Cu, Ag, Al_2O_3, and TiO_2 nanoparticles, Al_2O_3 gave the highest heat transfer rate at higher values of Rayleigh number.

Akbarinia and Behzadmehr [24] studied the influence of buoyancy force, centrifugal force and concentration of Al_2O_3 nanoparticles on convection heat transfer in horizontal curved tubes. For a given volume fraction of nanoparticles, buoyancy force caused a reduction in skin friction and at low Grashof number volume fraction had no visible effect on the skin friction.

To improve the cooling system performance in automobile car radiators, Hussein et al. [25] performed a numerical simulation to investigate the effect of cross-sectional area of the tube on friction factor and heat transfer by employing TiO_2-water nanofluid as coolants in radiators. Circular, elliptical, and flat tubes were the geometry consideration, and the flat tube showed the highest average heat transfer coefficient.

Peyghambarzadeh et al. [26] employed Al_2O_3 -water nanofluid as coolants with a range of volume concentration 0.1-1% in automobile radiators and up to 45% enhancement of heat transfer was obtained in comparison to the base fluid.

Ijam and Saidur [27] analyzed with SiC-water and TiO_2-water nanofluids as coolants in the mini-channel heat sink for the improvement of cooling performance in electronic devices. For a given volume concentration, SiC-water nanofluid gave a higher heat transfer rate compared to TiO_2-water nanofluid.

Clancy [28] experimented with nanofluid in the condenser of a vapor compression system for heat transfer enhancement and energy savings.

Firouzfar et al. [29] experimentally investigated the efficacy of a heat pipe heat exchanger in air conditioning systems by the suspension of silver nanoparticles in pure methanol. The sensible effectiveness was 5-22% for pure methanol whereas it was 9-32% for methanol-silver nanofluid.

Maghrebi et al. [30] investigated forced convection heat transfer of nanofluids in a porous channel and the effects of Lewis number, Schmidt number, and Brownian diffusion on heat transfer performance.

Harikrishnan and Kalaiselvam [31] experimented solidification and melting characteristics of TiO_2-melting palmitic acid nanofluid as Phase Change Material (PCM) for solar water heating systems. Enhancement of heat transfer was caused by the addition of nanoparticles in palmitic acid with different volume concentration.

Duangthongsuk and Wongwises [32] experimented heat transfer enhancement and pressure drop characteristics of TiO2-water nanofluid in a double-tube counter-flow heat exchanger and investigated the friction factor and heat transfer characteristics under turbulent flow with a range of Reynolds number 4000-18,000. They observed an increment of convective heat transfer coefficient with an increase of Reynolds number and mass flow rate of heating fluid in the heat exchanger.

γ-Al_2O_3-water and TiO_2-water nanofluids were used experimentally in a horizontal stainless steel shell and tube heat exchanger under turbulent flow conditions to study the effect of Peclet number, the volume concentration of suspended nanoparticles, and particle type on the forced convection heat transfer characteristics [33]. Significant improvement of heat transfer was observed with the addition of nanoparticles to the

base fluid at the same Peclet number and also the optimum volume concentration for both nanofluids was determined.

Fard et al. [34] carried out a numerical and experimental investigation of heat transfer of ZnO-water nanofluid as a hot stream in the concentric tube and plate heat exchanger and overall heat transfer coefficients in both heat exchangers were calculated as a function of hot and cold streams mass flow rates. The enhancement of heat transfer was 20% for the plate heat exchanger and 14% for the concentric heat exchanger.

Leong et al. [35] proposed a numerical model of shell and tube heat recovery exchanger operated with nanofluid-based coolants and achieved 7.8% of the heat transfer enhancement with the addition of 1% copper nanoparticles in ethylene-glycol-based fluid at a mass flow rate of 26.3 and 116.0 kg s^{-1} for flue gas and coolant respectively under laminar flow conditions. Gunnasegaran et al. [36] described a numerical model with three different types of nanofluids in ethylene glycol base fluid, namely copper, diamond, and silicon dioxide on an automobile flat tube plate-fin cross-flow compact heat exchanger considering 2% volume concentration and a single-phase approach. Variations of shear stress, skin friction, and convective heat transfer coefficient were studied and, improvement of thermal performance was shown with an increase of air and coolant Reynolds number.

Zamzamian et al. [37] experimented on forced convective heat transfer in a double pipe and plate heat exchanger under turbulent flow conditions using Al_2O_3 and CuO nanoparticles dispersed in ethylene glycol. Enhancement of the convective heat transfer coefficient was shown with an increase in particle volume concentration and nanofluid temperature. The heat transfer rate was increased by 2-50% compared to the base fluid and results were compared with theoretical calculations.

Kannadasan et al. [38] experimented horizontal and vertical helically coiled heat exchanger to compare the pressure drop and heat transfer characteristics with Cu-water nanofluid under turbulent flow conditions. Heat transfer enhancement was found more in the vertical heat exchanger and, friction factor increased with particle volume concentration. Pantzali et al. [39] worked with CuO-water nanofluid as coolant with 4% volume fraction to discover the effectiveness of plate heat exchanger and established that heat transfer augmentation was accomplished by addition of nanoparticles and

viscosity of nanofluid worked as an essential factor on the thermal performance of heat exchanger.

Pandey and Nema [40] applied a sine-shaped corrugated channel in a plate heat exchanger where Al_2O_3-water nanofluid was considered as a coolant, to investigate the heat transfer, frictional loss and pumping power with nanofluid volume concentration. The experimental results confirmed that for a given heat load, the volumetric flow rate of nanofluid decreased with significant pressure drop and improvement of heat transfer rate was maximum at 2% volume concentration of Al_2O_3 nanoparticles at a Peclet number of 7700.

Elias et al. [41] provided an analytical solution to observe the effect of different nanoparticle shapes on the enhancement of heat transfer and the thermodynamic performance of a shell and tube heat exchanger. Al_2O_3 nanoparticles of different shapes were dispersed in a water-ethylene glycol mixture. Cylindrical-shaped nanoparticles were found to be the optimum particle shape in the heat exchanger for better heat transfer performance.

Sonawane et al. [42] experimented Al_2O_3-water nanofluid on a concentric heat exchanger to study the average heat transfer rate. The convective heat transfer coefficient was improved with an increase of Reynolds number and particle volume concentration.

Pantzali et al. [43] explored the adequacy of nanofluids as coolants. It showed that the thermophysical properties were impressively influenced by adding nanoparticle to the base fluid. In such manner, a 4% CuO suspension in water is chosen. At that point, its performance on a plate heat exchanger (PHE) was considered. The examinations offered to ascend to the way that the flow in the exchanger additionally influences the coolant adequacy. In this manner, the liquid viscosity turns out to be the ultimate factor. In this way, nanofluids are not the reasonable substitution for large volume fraction.

Zhu et al. [44] introduced a novel one-stop technique for the planning of copper nanofluids from its related sulfide, $CuSO_4.5H_2O$ utilizing $NaH_2PO_2.H_2O$ in ethylene glycol under extremely light in the microwave scale. Highly non-agglomerated and highly stable nanofluids were acquired. The impacts of the diverse responding

operators, the complexes and the microwave irradiation were observed precisely under a transmission electron microscope (TEM) and associated infrared and sedimentary analysis. It was eventually observed to be a standout amongst the best and fast one-advance answer for getting ready Cu nanofluids.

Dongsheng et al. [45] worked ahead in regards to determining the various limiting factors to push ahead the development of nanofluids. It was taken up with a specific end goal to attach the stagnating extent of research in the field, since the time it had been detailed in regards to improved electrical conductivity.

Morteza et al. [46] researched the manufacture, the related thermal conductivity and the fluctuated rheological properties of nanofluids including copper nanoparticles in ethylene glycol base. The manufactured liquids displayed improved thermal conductivity. This was formed by directly forming the nanoparticles in the ethylene base fluid, utilizing assisted microwave heating. Which quickened the groups of metal to monodispersed nanostructures. The particles displayed an average size of 75 ± 25 nm for SEM micrographs, which aggregated to form spherical agglomerates within the size range of 300 nm. The various physicochemical properties, thermal conductivity, and viscosity included were measured in size range of 0.4-1.6 % weight fraction of nanoparticles within the range of 20-5- Celsius. The correlation models, suitable to the framework, was connected to think about the related properties which were somewhat observed to be higher if there should arise an occurrence of thermal conductivity improvement than the consistency partner. In this way, it demonstrated that with evolving focuses, the thermal properties show more articulated variety than on account of thickness.

Lin et al. [47] examined the warm execution of a level CPL, utilizing water-based and ethanol based Cu nanofluids under a few unfaltering sub-environmental working frameworks. This was finished with the evaporator of the CPL on a level plane set and bottom heated. Thus, the results showed that on the addition of Cu the evaporating heat coefficient gets highly enhanced along with the maximum heat removing the capacity of the system. However, there is an optimal concentration of the particles at which we observe the highest coefficient and, it decreases with further increase in the concentration. Along with the coefficient increases drastically with the operating

temperature of the system. The coefficient and the heat removal capacity consequently can be increased up to levels of 45% and 16% respectively when substituted with ethanol-based fluids.

Duangthongsuk et al. [48] experimented heat transfer enhancement and pressure drop characteristics of TiO_2-water nanofluid in a double-tube counter-flow heat exchanger and investigated the friction factor and heat transfer characteristics under turbulent flow with a range of Reynolds number 4000-18,000.

Williams et al. [49] experimentally explored the turbulent stream of alumina-water and zirconia-water nanofluids in tubes. They found that current connections for the single-stage stream can enough anticipate nanofluid stream convective heat exchange and weight drop.

Rea et al. [50] led an investigation on the laminar convective warmth exchange and weight drop of alumina–water and zirconia–water nanofluids in a tube with 4.5-mm inward width. Their discoveries demonstrated that, with appropriately measured nanofluid properties, there is no deviation in convective heat exchange and weight drop of nanofluid spill out of customary single-stage stream hypothesis.

Heris et al. [51] played out an exploratory investigation to decide the pressure drop and heat exchange qualities of Al_2O_3-water and CuO-water nanofluids in a triangular conduit under consistent heat flux where the flow was laminar. Their outcomes demonstrated that, at similar estimations of nanoparticle volume division and Reynolds number, utilizing Al_2O_3 nanoparticles is more beneficial than CuO nanoparticles. They numerically examined laminar constrained convective heat transfer condition. It was discovered that the nanofluid. Nusselt number increments with expanding molecule fixation and diminishing molecule width, and that the heat exchange upgrade turns out to be better at a higher Reynolds number in laminar flow utilizing nanofluids.

Akbarzadeh et al. [52] played out an affectability investigation on the nanofluid heat transfer in a wavy channel. Their outcomes showed that at a fixed Reynolds number (Re=600) and viewpoint proportion (0.1), the augmentation in the Nusselt number and the pressure drop up to 24% and 25%, separately, with an expansion in the active volume part of the nanoparticle.

Kayhani [53] researched the heat exchange conduit and pressure variety of water-based Al_2O_3 nanofluid coursing tentatively through a consistently warmed round pipe for turbulent administration. In this paper constant heat flux condition considered. The TiO_2 nanoparticle is having the ostensible breadth 15nm blended with distilled water. The analysis is done on volume focuses 0.1, 0.5, 1.0, 1.5 and 2.0 %. The outcomes demonstrate that for settled Reynolds number, heat exchange coefficient increments with the expansion in nanoparticle fixations. The Nusselt number expanded up to 8% for nanofluid with volume focus 2.0% at Reynolds number Re =11800.

Hamid et al. [54] explored the heat exchange coefficient and friction factor qualities of TiO_2 nanofluids. The constrained convection heated exchange is led at Reynolds number of 3000 to 24,000. The volume centralization of nanoparticles extended 0.5 to 1.5 % and physical properties were considered at temperature ran 30 to 70^oC. The outcomes were examined at three different temperatures 30, 50, 70^oC. The thickness and thermal conductivity of nanofluid expanded with volume fixation. For nanofluid fixation, 1.2%, the heat exchange coefficient has profound changes over the base liquid at temperature 30^oC.

In the literature, most of the studies focused on the enhancement of heat transfer utilizing nanofluid in different engineering applications. Very little information is available in the literature that deals with the pumping power issue of the nanofluid. Considering this fact, the scope of this thesis is to investigate the heat transfer characteristics and pumping power requirements of different water-based nanofluids (Al_2O_3, CuO and TiO_2) with different volume fractions through a right angle triangular shape corrugated tube. By the dispersion of nanoparticles in base fluid, the heat transfer rate is intensified but with the cost of pumping power. In the present numerical work, an optimum volume fraction for different nanofluids for a certain range of Reynolds number is obtained for which the nanofluid provides less pumping power compared to water. At a volume fraction, lower or higher than this optimum one, there is no or little advantage in reduction of pumping power as well as the mass flow rate of nanofluid. Finally, for the same heat transfer coefficient, reduction of pumping power, mass flow rate, and the volumetric flow rate of all three nanofluids are examined within a preferred particle volume fraction.

CHAPTER THREE

PHYSICAL MODEL AND BOUNDARY CONDITIONS

3.1 Physical Model

A corrugated tube with a constant heat flux on its surface can be considered as the least complicated case to investigate heat transfer rate and corresponding pumping power requirement. To investigate the performance of Nanofluid in a corrugated tube, a numerical study has been carried out by employing commercial computational fluid dynamics software ANSYS Fluent. 2D simulation with the axisymmetric model is considered for analyzing different parameter which is shown in Fig. 3.1. Turbulent flow through a corrugated tube of 8 mm diameter and 200 mm length is presented with a constant heat flux of 5000 W/m^2, which is applied at the wall boundary of the corrugated tube. The corrugation has an amplitude of 1.60 mm and a wavelength of 6 mm. Realizable k-ε turbulent model is employed with enhanced wall treatment for the analysis. Nanofluid is allowed to flow with uniform velocity and uniform temperature of 300 K at the inlet of the tube with an assumption of a no-slip condition. All the fluid dynamic and heat exchange parameters are extricated after the hydrodynamic and thermal improvement of the fluid stream, and in this case, the entrance length is x/D=20 beyond which all the measurements are taken.

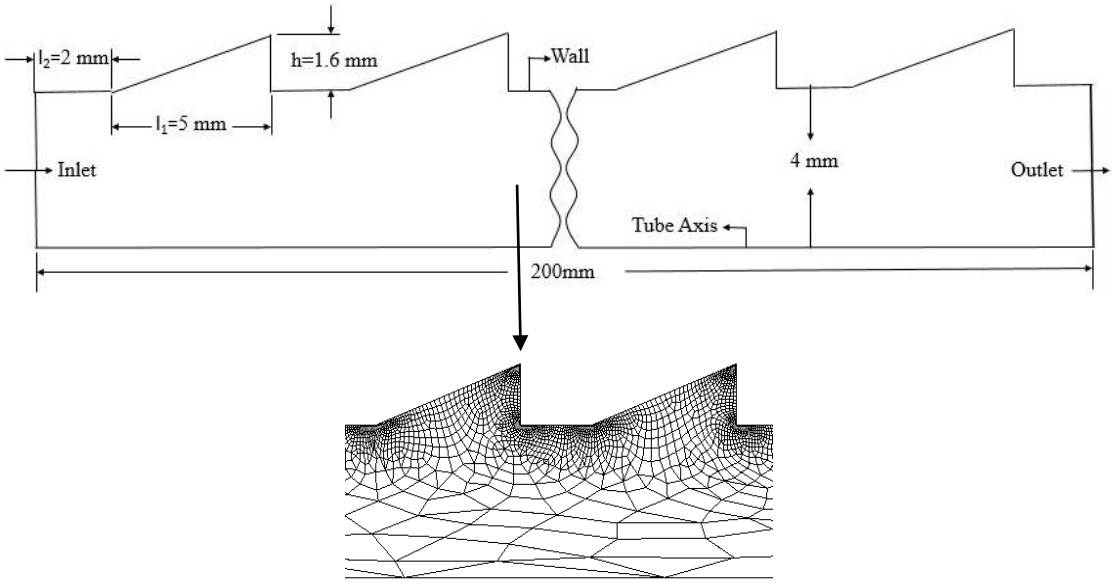

Figure 3.1 Numerical domain of the right-angled triangular corrugated pipe and corresponding mesh (not to scale)

CHAPTER FOUR

METHODOLOGY

4.1 Governing Equations

The governing equations for continuity, momentum, and energy for forced convection under turbulent flow and steady-state conditions are expressed as follows:

Continuity equation:

$$\frac{\partial}{\partial x_i}(\rho u_i) = 0 \tag{5.1}$$

Momentum equation:

$$\frac{\partial(\rho u_i u_j)}{\partial x_j} = -\frac{\partial p}{\partial x_i} + \frac{\partial}{\partial x_j}\left[\mu\left(\frac{\partial u_i}{\partial x_j} + \frac{\partial u_j}{\partial x_i}\right)\right] + \frac{\partial}{\partial x_j}(-\rho\overline{u_i' u_j'}) \tag{5.2}$$

Energy equation:

$$\frac{\partial}{\partial x_i}(-\rho u_i T) = \frac{\partial}{\partial x_j}\left((\Gamma + \Gamma_t)\frac{\partial T}{\partial x_j}\right) \tag{5.3}$$

Here Γ is molecular thermal diffusivity, and Γ_t is turbulent thermal diffusivity which can be expressed as:

$$\Gamma = \frac{\mu}{Pr'}$$

$$\Gamma_t = \frac{\mu_t}{\mathrm{Pr}_t'}$$

The normal Reynolds stress which is combined by Boussinesq relationship and the eddy viscosity definition is given by:

$$(-\rho\overline{u_i' u_j'}) = \mu_t\left(\frac{\partial u_i}{\partial x_j} + \frac{\partial u_j}{\partial x_i}\right) \tag{5.4}$$

The realizable *k-ε* model is considered to model turbulent eddy viscosity and transport equation for turbulent kinetic energy and turbulent dissipation rate which has been derived from an exact equation for the transport of the mean-square vorticity fluctuation.

Turbulent eddy viscosity is defined as:

$$\mu_t = \rho C_\mu \frac{k^2}{\varepsilon}$$

Turbulent kinetic energy:

$$\frac{\partial}{\partial t}(\rho k)+\frac{\partial}{\partial x_j}(\rho k u_j)=\frac{\partial}{\partial x_j}\left[\left(\mu+\frac{\mu_t}{\sigma_k}\right)\frac{\partial k}{\partial x_j}\right]+G_k+G_b-\rho\varepsilon-Y_M+S_k \qquad 5.5$$

Turbulent dissipation rate:

$$\frac{\partial}{\partial y}(\rho\varepsilon)+\frac{\partial}{\partial x_j}(\rho\varepsilon u_j)=\frac{\partial}{\partial x_j}\left[\left(\mu+\frac{\mu_t}{\sigma_\varepsilon}\right)\frac{\partial \varepsilon}{\partial x_j}\right]+\rho C_1 S\varepsilon-\rho C_2\frac{\varepsilon^2}{k+\sqrt{\nu\varepsilon}}+C_{1\varepsilon}\frac{\varepsilon}{k}C_{3\varepsilon}G_b+S_\varepsilon \qquad 5.6$$

Where

$$C_1=\max\left[0.43,\frac{\eta}{\eta+5}\right],\ \eta=S\frac{k}{\varepsilon}\ \text{and}\ S=\sqrt{2S_{ij}S_{ij}}$$

Here G_k represents the generation of turbulent kinetic energy due to the mean velocity gradients, G_b is the generation of turbulent kinetic energy due to buoyancy, Y_M represents the contribution of the fluctuating dilatation in compressible turbulence to the overall dissipation rate, and σ_k and σ_ε are the turbulent Prandtl for k and ε respectively.

4.2 Thermal and Fluid Dynamic Properties

The Reynolds number for the flow of nanofluid is expressed as:

$$Re=\frac{\rho_{nf}U_{av}D_h}{\mu_{nf}}$$

The rate of heat transfer Q_{nf} to the tube wall is assumed to be wholly dissipated to nanofluid flowing through a circular tube, raising its temperature from inlet fluid bulk temperature T_{bi} to exit fluid bulk temperature T_{bo}. Thus,

$$Q_{nf}=m_{nf}C_{P_{nf}}\left(T_{bo}-T_{bi}\right) \qquad 5.7$$

Where m_{nf} the mass flow rate of nanofluid is, $C_{p_{nf}}$ is the specific heat of nanofluid at constant pressure. The definition of bulk temperatures T_b is given by:

$$T_b=\frac{\int_0^R uTdA_c}{\int_0^r udA_c} \qquad 5.8$$

A_c is a cross-sectional area of the circular section. The average heat transfer coefficient h_c is given by:

$$h_c=\frac{Q_{nf}}{A_w\left(\Delta T_m\right)}$$

Where A_w is the surface area of the circular tube and the temperature difference between the wall, and the fluid is calculated as:

$$\Delta T_m = \left(T_w - T_b\right) \tag{5.9}$$

So the expression of average Nusselt number is defined as follows:

$$Nu = \frac{h_c D_h}{K_{nf}} \tag{5.10}$$

The pumping power per unit length in turbulent flow is given by:

$$W = \frac{\left(\pi / 4\right) D_h{}^2 U_{av} \Delta P}{L} \tag{5.11}$$

4.3 Friction Factor

The friction factor, or also called the Darcy friction factor is defined as:

$$f = \frac{\Delta P\left(\frac{D_h}{L}\right)}{\left(\frac{\rho U_{av}^2}{2}\right)} \tag{5.12}$$

Where ΔP is the pressure drop, L is the length of the pressure drop test section, ρ is the fluid density and U is the average velocity of the flow. The pressure drop equation in a horizontal pipe can be written as:

$$\Delta P = \frac{fL\rho U_{av}^2}{2D_h} \tag{5.13}$$

4.4 Thermophysical Properties of Nanofluids

In this study Al_2O_3, CuO, and TiO_2 nanoparticles of the diameter of 50 nm are considered to be dispersed in water as the base fluid. The properties of the base fluid and the nanoparticles are given in Table 4.1.

The useful thermophysical properties of different nanofluids have been calculated using different empirical equations which are given as follows.

Table 4.1 Thermophysical properties of water and nanoparticles

Chemical compound	Density (kg m^{-3})	Specific heat (J kg^{-1} K^{-1})	Thermal conductivity (W m K^{-1})	Viscosity (N s m^{-2})
Water	996.59	4179.2	0.6102	0.000892
Al_2O_3	3970	775	39	_
TiO_2	4000	711	8.04	_
CuO	6500	525	17.65	_

4.4.1 Dynamic viscosity

Compared with the experimental studies on thermal conductivity of nanofluids, there are limited rheological studies reported in the literature for viscosity. Different models of viscosity have been used by researchers to model the effective viscosity of nanofluid as a function of volume fraction. There are several equations for dynamic viscosity. Among them, we use Pak and Cho [55] equation for TiO_2 and Maiga et al. [56] equations for Al_2O_3. Since there are no experimental results available in the literature for the viscosity of CuO-water nanofluid at different volume fraction where base fluid is water, the correlation developed by Corcione [57] has been used. The equation can be expressed as:

For TiO_2–water nanofluid:

$$\mu_{nf} = \mu_F (1.0623 + 4.7037\phi + 167.74\phi^2) \tag{5.14}$$

For Al_2O_3–water nanofluid:

$$\mu_{nf} = \mu_f (1 + 7.3\phi + 123\phi^2) \tag{5.15}$$

For CuO–water nanofluid:

$$\frac{\mu_{nf}}{\mu_{bf}} = \frac{1}{1 - 34.87\left(d_p / d_{bf}\right)^{-0.3} \phi^{1.03}} \tag{5.16}$$

Where d_{bf} is the equivalent diameter of the base fluid molecule and is given by:

$$d_{bf} = \left[\frac{6M}{N\pi\rho_{fo}}\right]^{1/3}$$

Where M is the molecular weight of the base fluid, N is the Avogadro number, and ρ_{fo} is the mass density of the base fluid calculated at temperature T_o = 293 K.

4.4.2 Thermal conductivity

A wide range of experimental and theoretical studies were conducted in the literature to the model thermal conductivity of nanofluids. The existing results was generally based on the definition of the effective thermal conductivity of a two-component mixture. There are several thermal conductivity equations among them we use Pak and Cho [55] equation for TiO_2 and Al_2O_3. Moreover for CuO-water nanofluid we have used the Maxwell [58] model. The following formulas are given by

For TiO_2–water nanofluid:

$$k_{nf} = k_{bf}\left(1.0084 + 2.1796\phi\right) \tag{5.17}$$

For Al_2O_3–water nanofluid:

$$k_{nf} = k_{bf}\left(1.0021 + 7.3349\phi\right) \tag{5.18}$$

For CuO–water nanofluid:

$$k_{nf} = \frac{k_p + 2k_{bf} + 2\left(k_p - k_{bf}\right)\phi}{k_p + 2k_{bf} - \left(k_p - k_{bf}\right)\phi} k_{bf} \tag{5.19}$$

4.4.3 Density

Using classical formulas derived for a two-phase mixture density developed by Xuan et al. [59] of the nanofluid as a function of the particle volume concentration and individual properties can be computed using the following equation:

$$\rho_{nf} = \rho_{bf}\left(1-\phi\right) + \rho_p\phi \tag{5.20}$$

4.4.4 Specific heat

The specific heat capacity developed by Pak and Cho [55] of the nanofluid as a function of the particle volume concentration and individual properties can be computed using the following equation:

$$C_{nf} = C_{bf}\left(1-\phi\right) + C_p\phi \tag{5.21}$$

Now the Thermophysical Properties of the different Nanofluids are given in table 4.2, table 4.3, and table 4.4

Table 4.1 Thermophysical Properties of Al_2O_3 – Water Nanofluid

Property	1%	2%	3%	4%	5%
Density (ρ)	1026.3241	1056.0582	1085.7923	1115.5264	1145.2605
Thermal Conductivity (κ)	0.6562	0.7010	0.7458	0.7905	0.8353
Specific Heat (C_p)	4145.158	4111.116	4077.074	4043.032	4008.99
Viscosity (μ)	0.000968	0.001066	0.001186	0.001328	0.001492

Table 4.2 Thermophysical Properties of TiO_2 – Water Nanofluid

Property	1%	2%	3%	4%	5%
Density (ρ)	1026.6241	1056.6582	1086.6923	1116.7264	1146.7605
Thermal Conductivity (κ)	0.6286	0.6419	0.6552	0.6685	0.6818
Specific Heat (C_p)	4144.518	4109.836	4075.154	4040.472	4005.79
Viscosity (μ)	0.001004	0.001091	0.001208	0.001355	0.001531

Table 4.3 Thermophysical Properties of CuO – Water Nanofluid

Property	1%	2%	3%	4%	5%
Density (ρ)	1051.6241	1106.6582	1161.6923	1216.7264	1271.7605
Thermal Conductivity (κ)	0.6267	0.6438	0.6612	0.6788	0.6968
Specific Heat (C_p)	4142.658	4106.116	4069.574	4033.032	3996.49
Viscosity (μ)	0.000959	0.001042	0.001142	0.001264	0.001417

CHAPTER FIVE

CODE VALIDATION ANALYSIS

5.1 Code Validation Test

Numerical study of heat transfer behavior and pumping power requirement for the flow of fluid through the plain circular tube, commercial computational fluid dynamics software – ANSYS Fluent has been employed in the present work. A flow of water with uniform velocity and a range of Reynolds number of 5000 to 25000 has been considered and the calculated Nusselt numbers at the fully developed zone are validated with the values of Nusselt number obtained from the correlation which is developed by Notter and Sleicher [59]. From figure 5.1 it has been observed that the two results are very close to each other.

The correlation developed by Notter and Sleicher is as follows:

$$N_u = 5 + 0.016\,\mathrm{Re}^a\,\mathrm{Pr}^b$$

Where,

$$a = 0.88 - \frac{0.24}{4+\mathrm{Pr}} \text{ and } b = 0.33 + 0.5e^{-0.6\mathrm{Pr}}$$

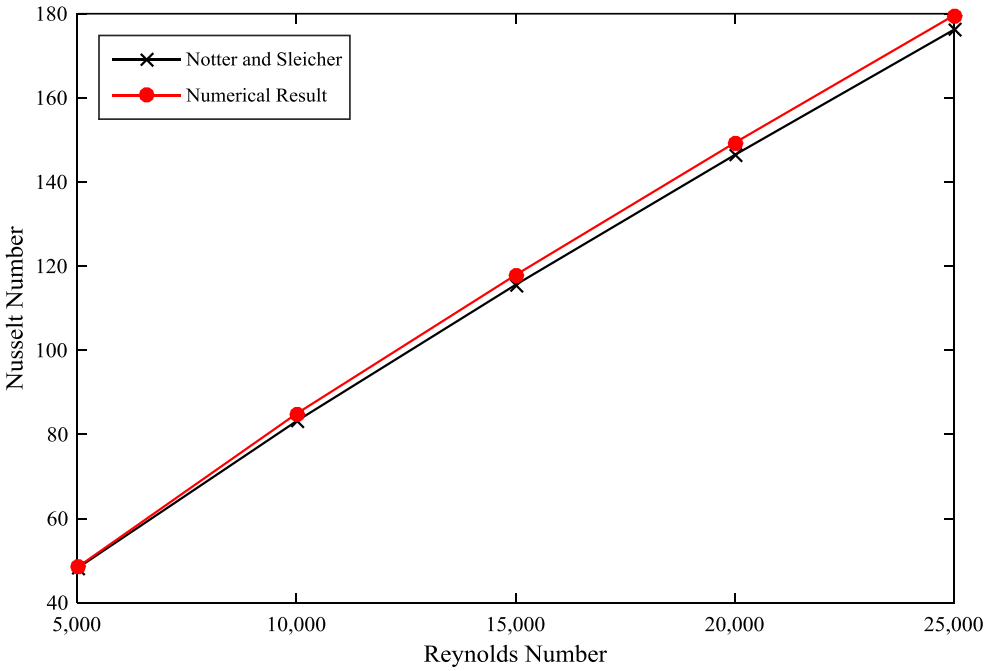

Figure 5.1 Comparison of Nusselt number between Notter and Sleicher and present work for different Reynolds number.

5.2 Grid Independence Test

For the grid independence study, the working substance has been taken as water, and the simulation was run at Re = 5,000. Grid independence test was carried out to discover the optimum grid size for the present study. Six different grid sizes like 8419, 14115, 18959, 24397, 30042 and 35763 were tested to find out the effect on the Nusselt number calculated at a distance of 199 mm from the inlet of the tube. It has been found that there is no significant change in Nusselt number beyond the grid size of 24397, which is shown in figure 5.2. Therefore, for the present study, the grid size of 24397 has been used to perform all the simulations.

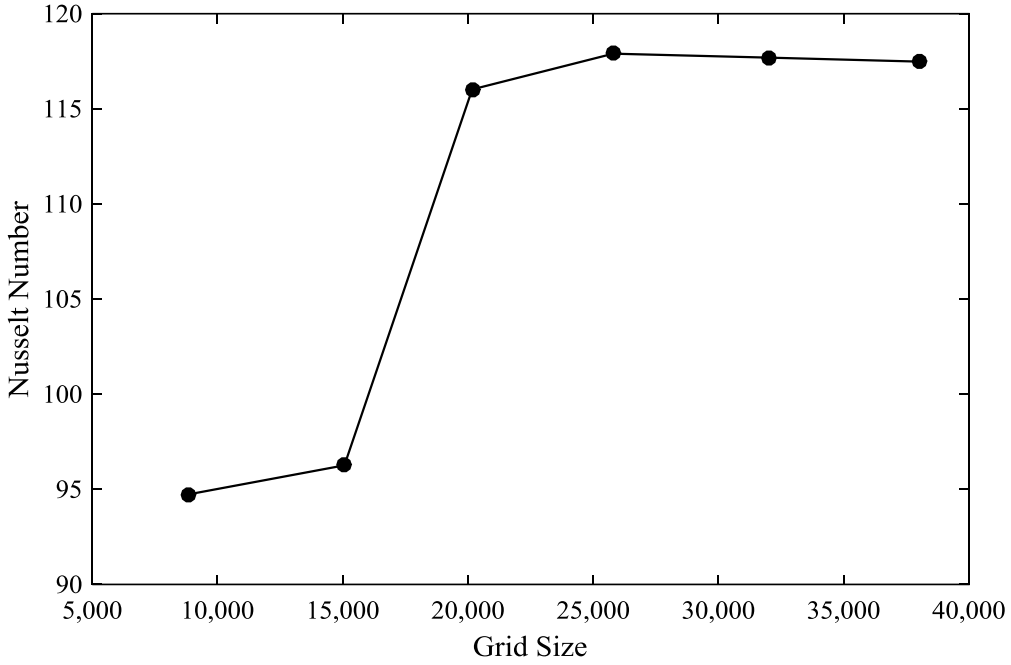

Figure 5.2 Comparison of Nusselt number for different grid sizes.

CHAPTER SIX

RESULTS AND DISCUSSIONS

6.1 Effect of Geometrical Parameter

Initially, geometry has been selected where l_1, l_2, and h are 4 mm, 2 mm and 1.60 mm respectively for measuring convective heat transfer coefficient using different nanofluid (CuO, Al_2O_3 and TiO_2) in a right-angled triangular shaped corrugated tube for turbulent flow. However, to find out the maximum effective heat transfer coefficient, Nusselt number has been calculated by varying the parameters which are l_1, l_2, and h respectively using water as the base fluid. First of all Nusselt number is calculated by varying one parameter (l_1) and other two parameters (l_2 and h) remain constant, which are characterized as a case number. For case number VIII, where the length l_1 is 5 mm the highest value of Nusselt number is found which is shown in table 6.1.

Table 6.1 Nusselt number at a different length (l_1)

Case No	l_2 (mm)	h (mm)	l_1 (mm)	Nu (Using Only Water) at Re=25000
Case I	2	1.6	2	208.77
Case II	2	1.6	2.25	202.95
Case III	2	1.6	2.5	200.47
Case IV	2	1.6	3	201.08
Case V	2	1.6	3.25	202.95
Case VI	2	1.6	3.5	206.14
Case VII	2	1.6	4	214.22
Case VIII	2	1.6	5	219.97
Case IX	2	1.6	7	217.78

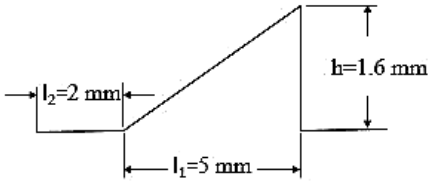

From figure 6.1 it has been observed that the Nusselt number is decreasing with the increase in length (l_1) up to 2.5 mm. It is occurred due to the increase of corrugation. As the number of corrugation increases, the corrugated tube works like a plain tube. However, after 2.5 mm the Nusselt number is going to increase up to 5 mm length. But beyond the length of 5 mm, the Nusselt number is again going to decrease. Which is happened due to the decrease of corrugation. As the number of corrugation decreases,

the corrugated tube works like a plane tube as well as less vorticity occurred in corrugation. So at the length of 5 mm, the highest value of Nusselt number is found.

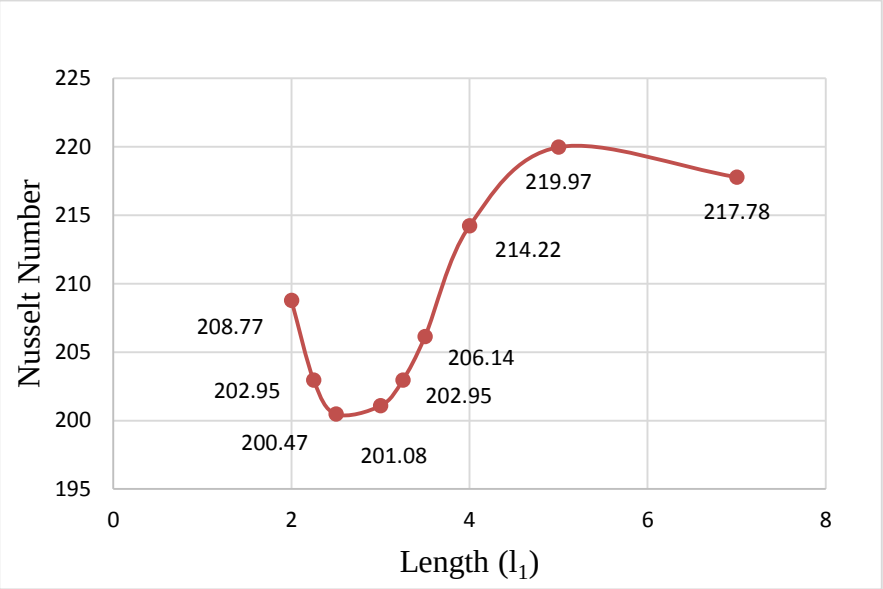

Figure 6.1 Nusselt number at different length l_1 when the other two parameters (l_2 and h) remain constant

Now the Nusselt number is calculated by varying one parameter (l_2), and other two parameters (l_1 and h) remain constant as 4 mm and 1.6 mm respectively for the case number VII, X and XI. From figure 6.2, it has been observed that the Nusselt number is decreasing by decreasing the length. However, if the length l_1 and height h is 5 mm and 1.60 mm respectively then the maximum value of Nusselt number is found in case of VIII which is shown in table 6.2.

Table 6.2 Nusselt number at a different length (l_2)

Case No	l_1 (mm)	h (mm)	l_2 (mm)	Nu (Using Only Water) at Re=25000
Case VIII	5	1.6	2	219.97
Case VII	4	1.6	2	214.22
Case X	4	1.6	1.5	210.78
Case XI	4	1.6	1	206.79

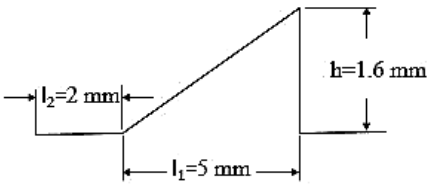

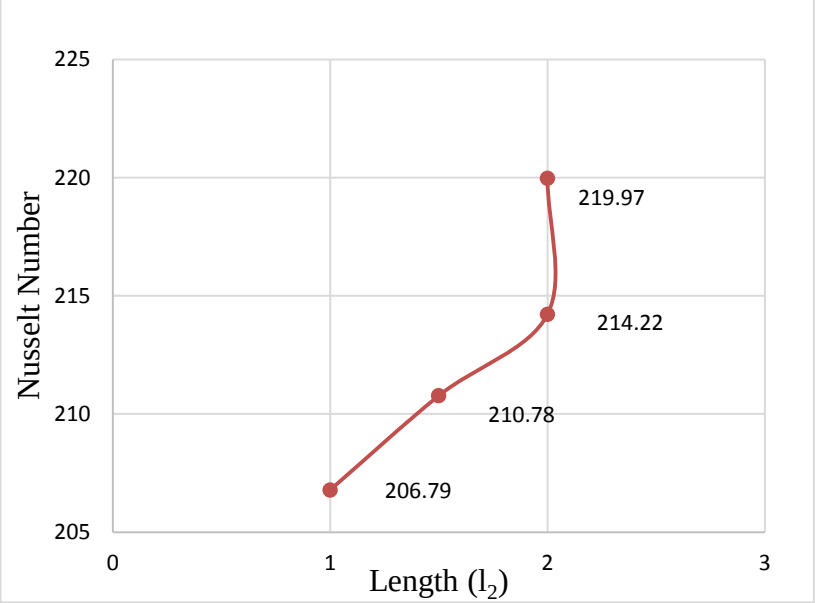

Figure 6.2 Nusselt number at different length l_2 when the other two parameters (l_1 and h) remain constant

Finally, the Nusselt number is calculated by varying the last parameter (h), and other two parameters (l_1 and l_2) remain constant as 4 mm and 2 mm respectively for the case number VII, XII and XIII. From figure 6.3, it has been observed that the Nusselt number is decreasing by decreasing the height. However, if the length l_1 and l_2 are 5 mm and 2 mm respectively then the maximum value of Nusselt number is found in case of VIII which is shown in table 6.3. So for our study, the useful geometry is case VIII where the three parameters (l_1, l_1, and h) are 5 mm, 2 mm and 1.60 mm.

Table 6.3 Nusselt number at different heights (h)

Case No	l_1 (mm)	l_2 (mm)	h (mm)	Nu (Using Only Water) at Re=25000
Case VIII	5	2	1.6	219.97
Case VII	4	2	1.6	214.22
Case XII	4	2	1.1	206.14
Case XIII	4	2	0.6	204.85

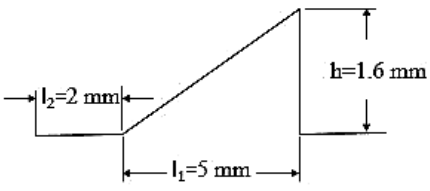

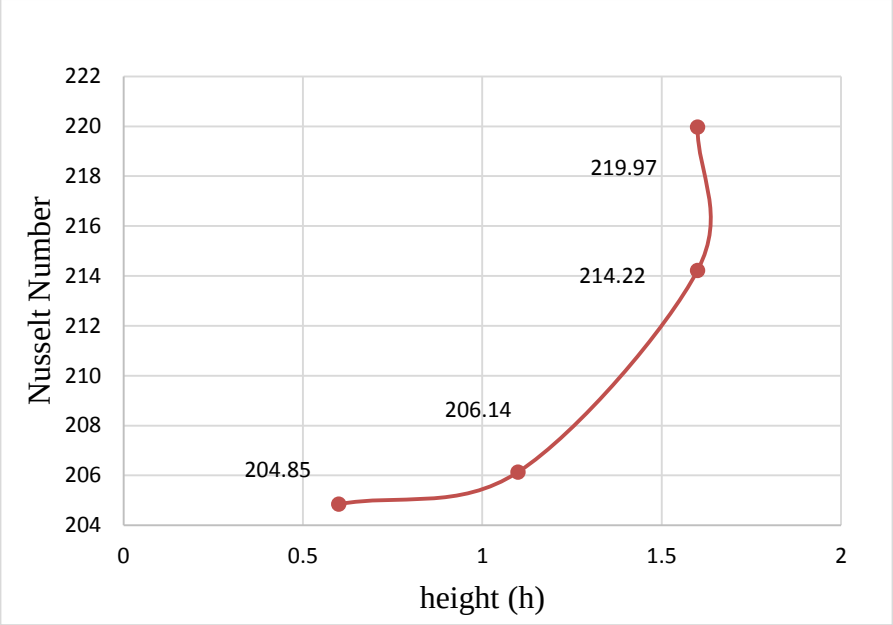

Figure 6.3 Nusselt number at different height h when the other two parameters (l_1 and l_2) remain constant

6.2 Nusselt Number for Different Volume Fraction of Nanofluid

The figure 6.4, 6.5 and 6.6 show the effect of volume fraction and Reynolds number on the Nusselt number for Al_2O_3-water, CuO–water and TiO_2-water respectively. From the figure, it is obvious that the Nusselt number of all the nanofluids used in the present work increases with the increase in Reynolds number and volume fraction of the nanofluids. Which is occurred because of the increment of the effective thermal conductivity and an increase of energy exchange rate resulting from the irregular and chaotic motion of ultrafine particles of the nanofluids with the increases of the volume fraction as well as increment of convection with the increase in Reynolds number. Generally, a higher Reynolds number corresponds to higher fluid velocity and temperature gradient, which in turn results in a higher value of Nusselt number.

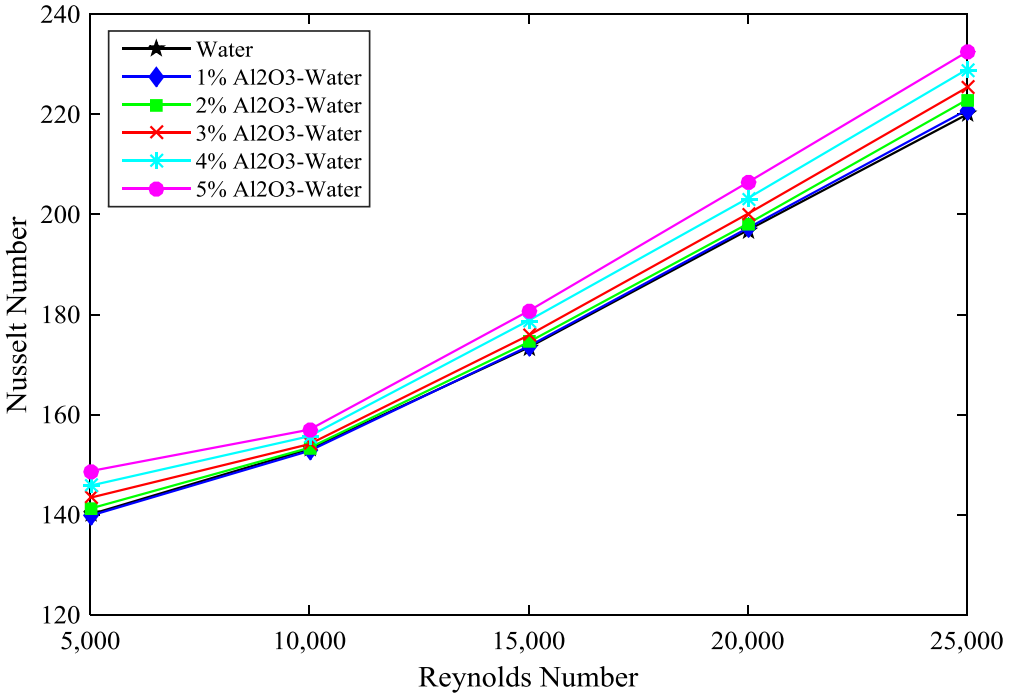

Figure 6.4 Comparison of Nusselt Number for the different volume fraction of Al_2O_3-Water nanofluid.

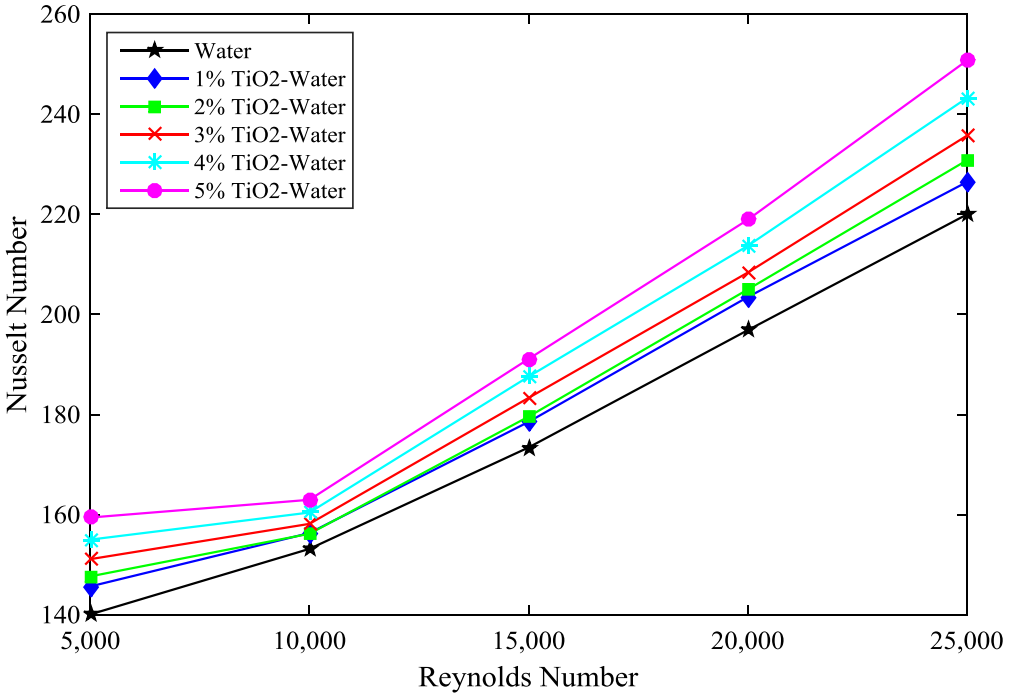

Figure 6.5 Comparison of Nusselt Number for the different volume fraction of TiO_2-Water nanofluid.

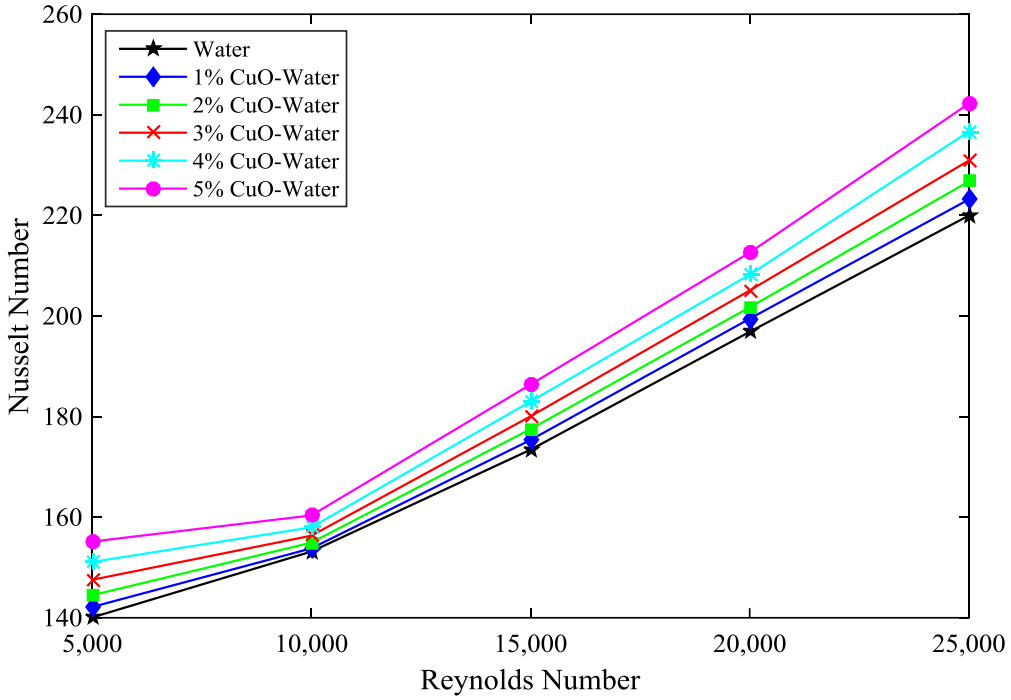

Figure 6.6 Comparison of Nusselt Number for the different volume fraction of CuO-Water nanofluid.

6.3 Nusselt Number at Constant Volume Fraction of Nanofluid

Figure 6.7, 6.8, 6.9, 6.10 and 6.11 show the comparison of Nusselt number at a constant volume fraction of different nanofluids. From the following figures, it has been observed that for the constant volume fraction of nanofluid the Nusselt number is increasing with the increase in Reynolds number for all nanofluids. From the figures, it is evident that TiO_2-water gives more enhancement of Nusselt number that the other two nanofluids and Al_2O_3-water gives less enhancement of Nusselt number than the other two nanofluids. The enhancement of Nusselt number at 1% volume fraction of Al_2O_3-water, TiO_2-water, and CuO-water is 0.40%, 2.95%, and 1.45% respectively than that of water. Similarly, the enhancement of Nusselt number at 5% volume fraction of Al_2O_3-water, TiO_2-water, and CuO-water is 5.68%, 13.98%, and 10.12% respectively than that of water.

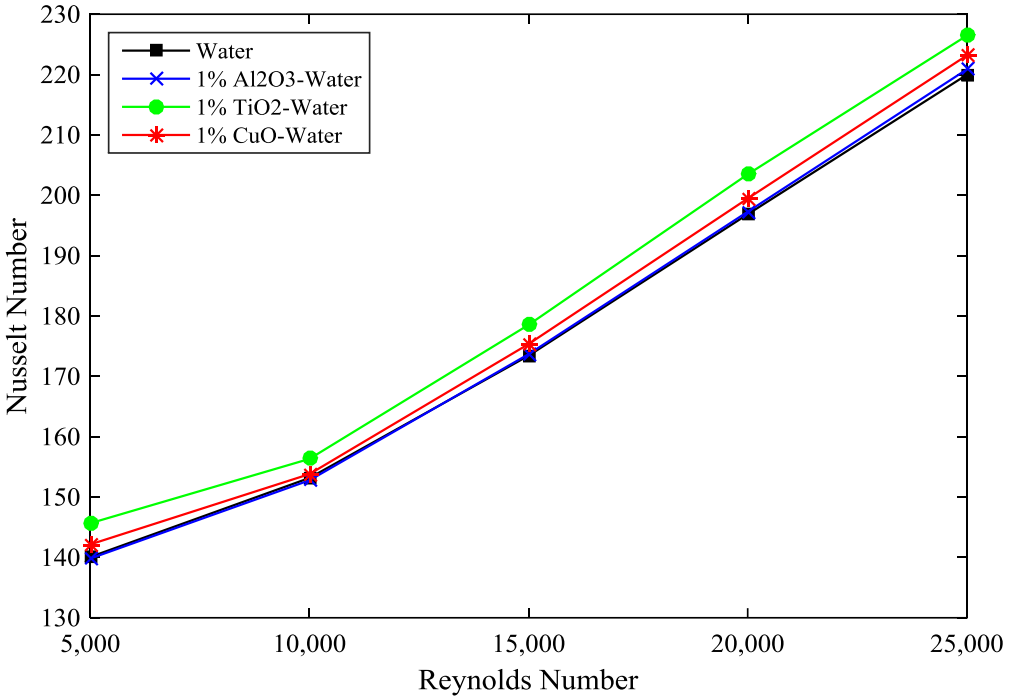

Figure 6.7 Comparison of Nusselt Number at 1% volume fraction of nanofluids.

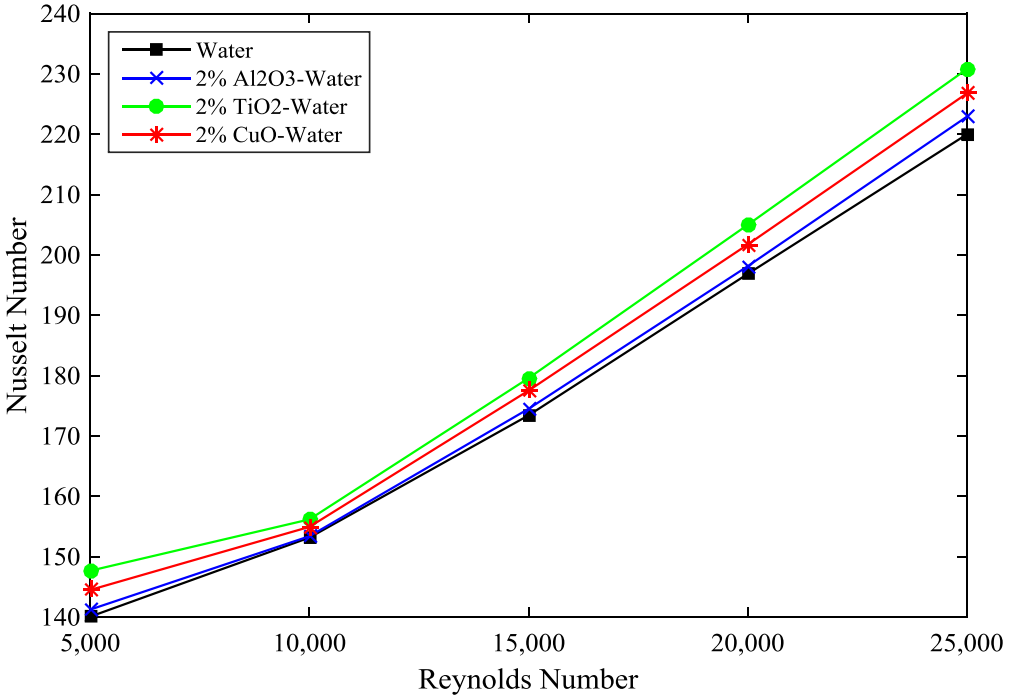

Figure 6.8 Comparison of Nusselt Number at 2% volume fraction of nanofluids.

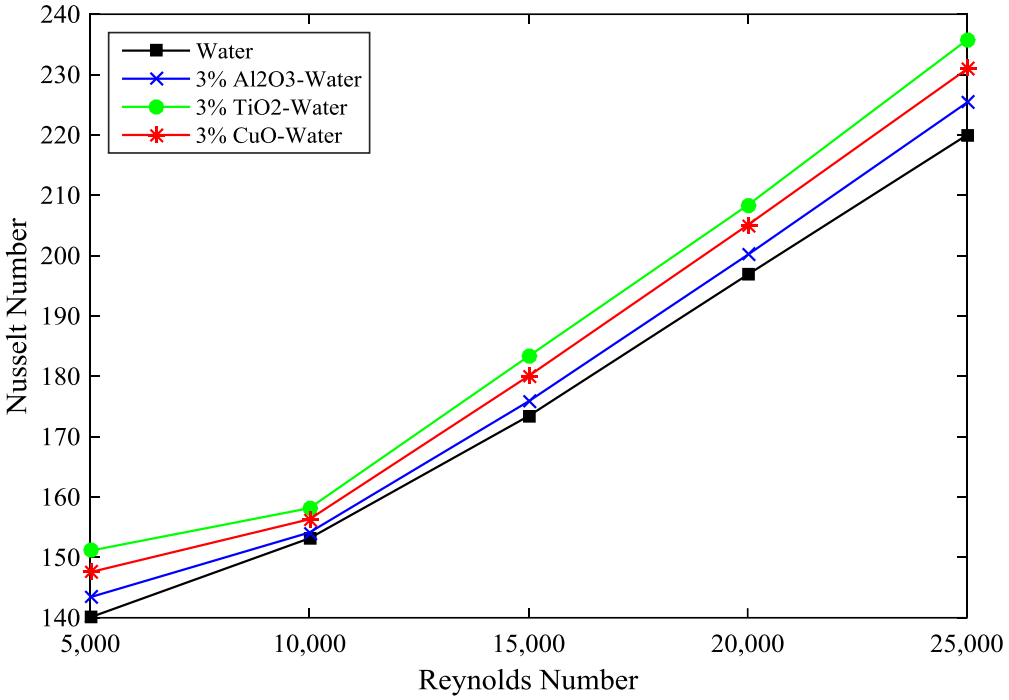

Figure 6.9 Comparison of Nusselt Number at 3% volume fraction of nanofluids.

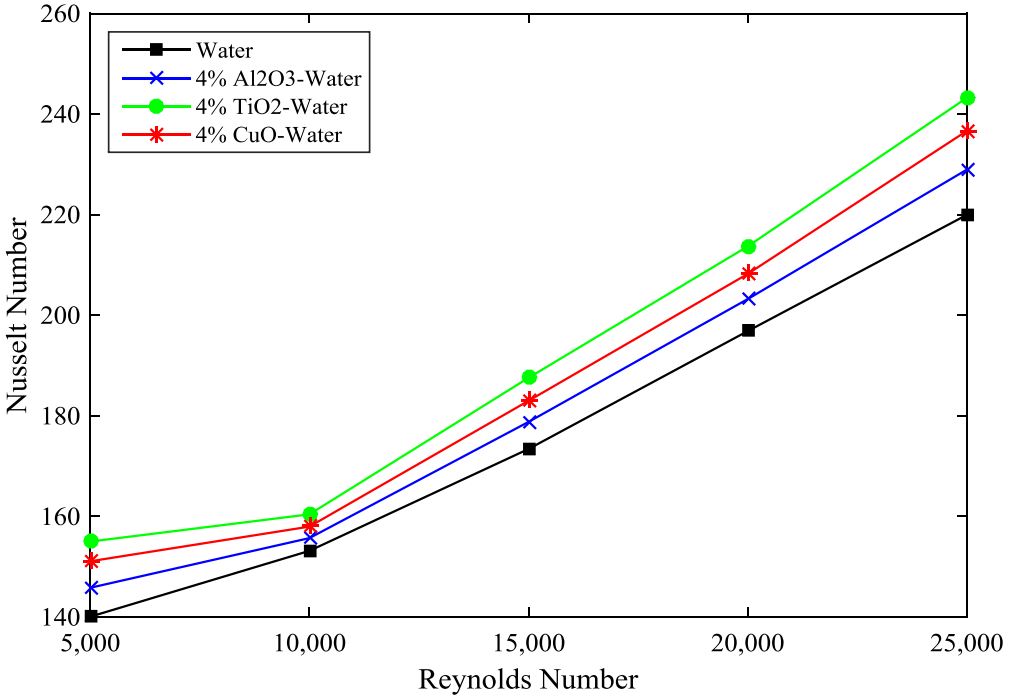

Figure 6.10 Comparison of Nusselt Number at 4% volume fraction of nanofluids.

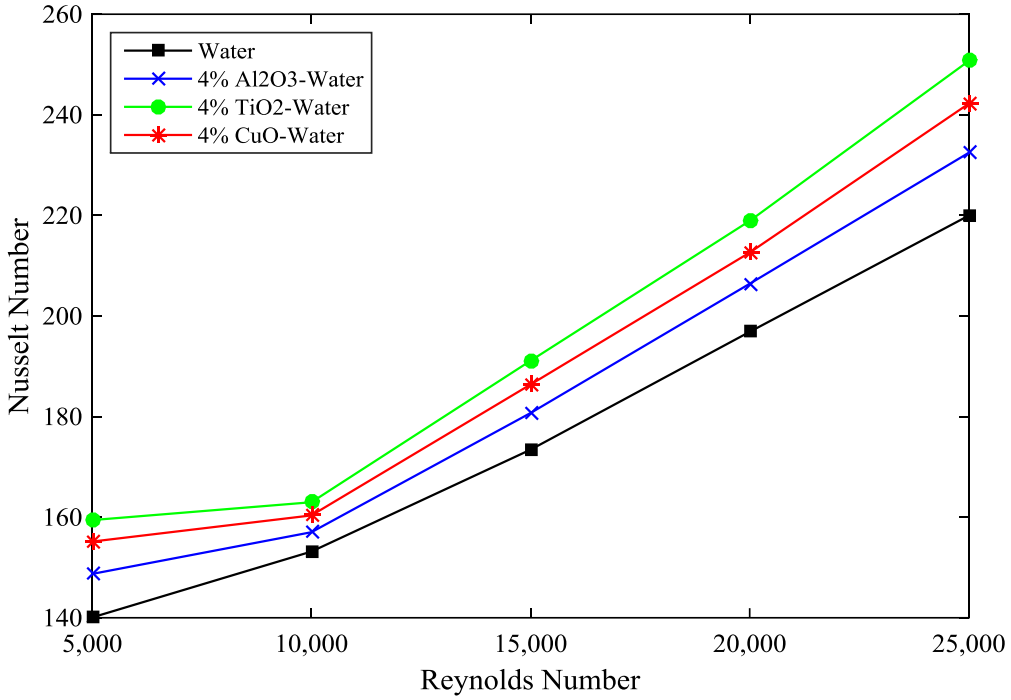

Figure 6.11 Comparison of Nusselt Number at 5% volume fraction of nanofluids.

6.4 Heat Transfer Coefficient for Different Volume Fraction of Nanofluid

The figure 6.12, 6.13 and 6.14 represent the effect of volume fraction of nanofluids on heat transfer coefficient at different Reynolds number. From the figures, it is observed that the value of heat transfer coefficient increases with the increase in volume fraction and Reynolds number. Which is due to the increases of the thermal conductivity and decreases of the specific heat capacity of the nanofluids which increases the Nusselt number with higher velocity and temperature gradient, and this phenomenon increases the heat transfer coefficient gradually.

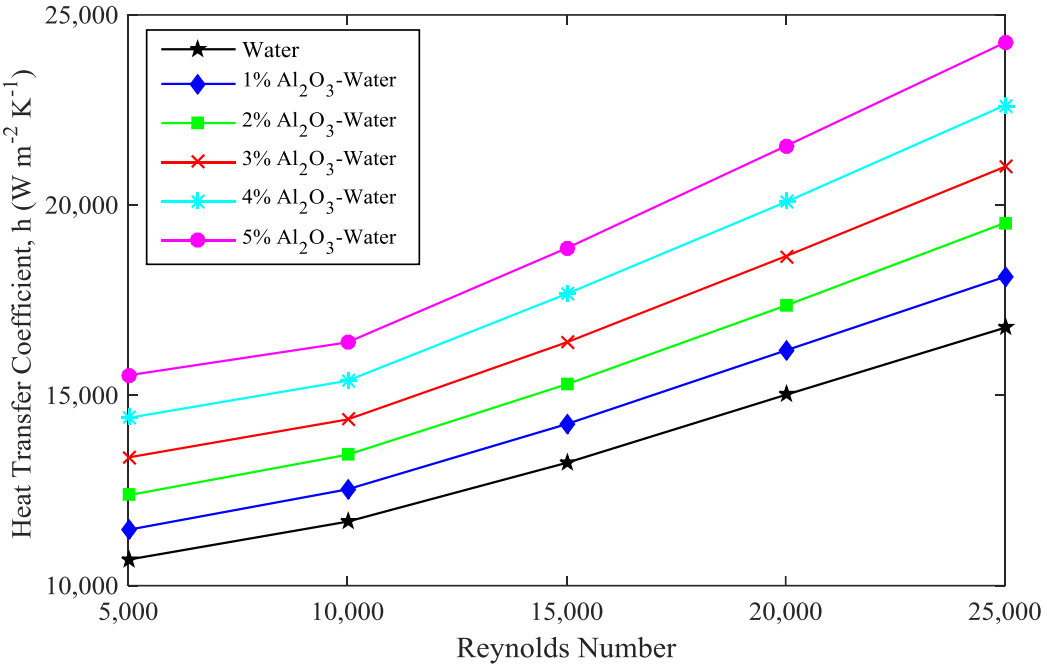

Figure 6.12 Comparison of Heat Transfer Coefficient for the different volume fraction of Al_2O_3-Water nanofluid.

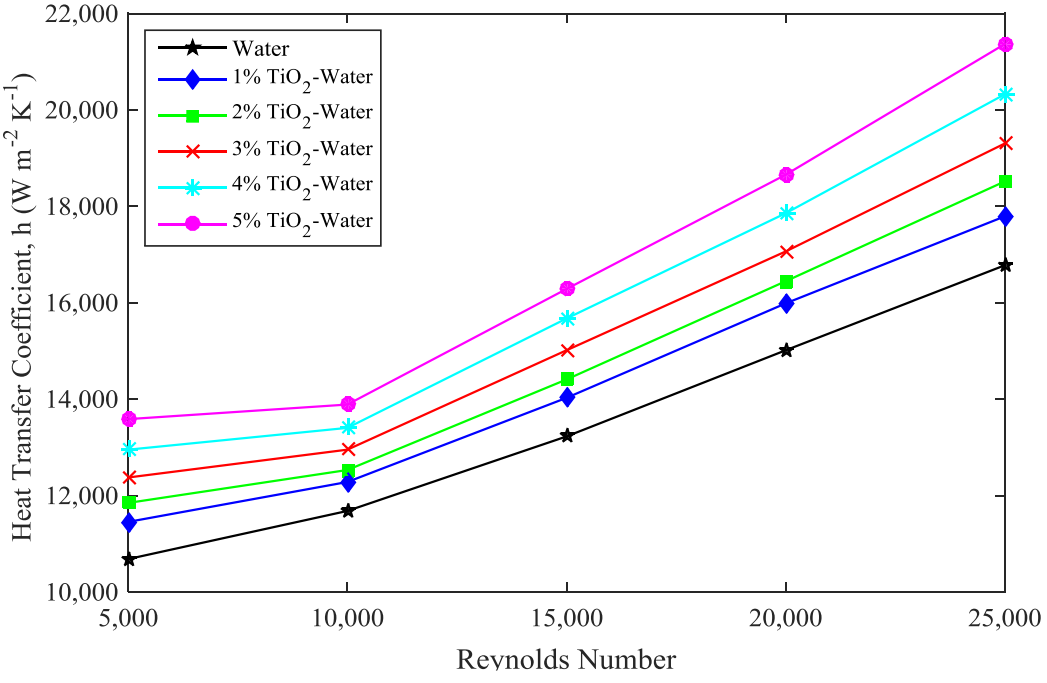

Figure 6.13 Comparison of Heat Transfer Coefficient for the different volume fraction of TiO_2-Water nanofluid.

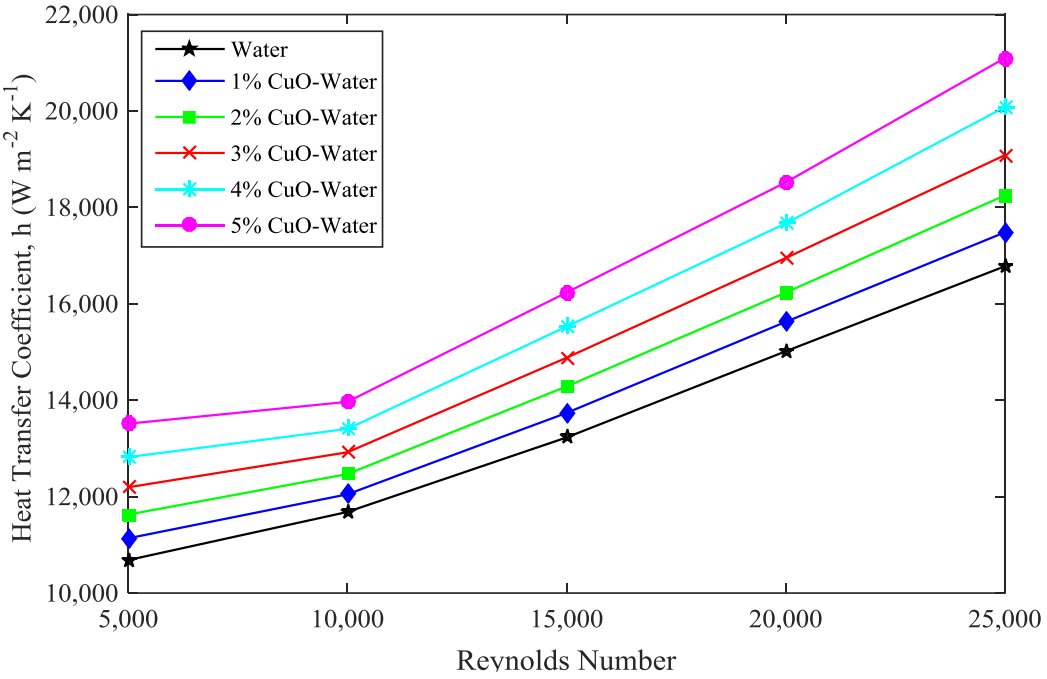

Figure 6.14 Comparison of Heat Transfer Coefficient for the different volume fraction of CuO-Water nanofluid.

6.5 Heat Transfer Coefficient at Constant Volume Fraction of Nanofluid

Figures 6.15, 6.16, 6.17, 6.18 and 6.19 indicate the effect of heat transfer coefficient on Al_2O_3-water, TiO_2-water, and CuO-water nanofluids at a constant volume fraction of 1% to 5%. From the figures, it has been observed that Al_2O_3-water nanofluid shows more enhancement than the other nanofluids where TiO_2-water and CuO-water show almost similar enhancement. The enhancement of heat transfer coefficient at 1% volume fraction of Al_2O_3-water, TiO_2-water, and CuO-water is 7.97%, 6.05%, and 4.20% respectively than that of water. Similarly, the enhancement of heat transfer coefficient at 5% volume fraction of Al_2O_3-water, TiO_2-water, and CuO-water is 44.66%, 27.35%, and 25.74% respectively than that of water.

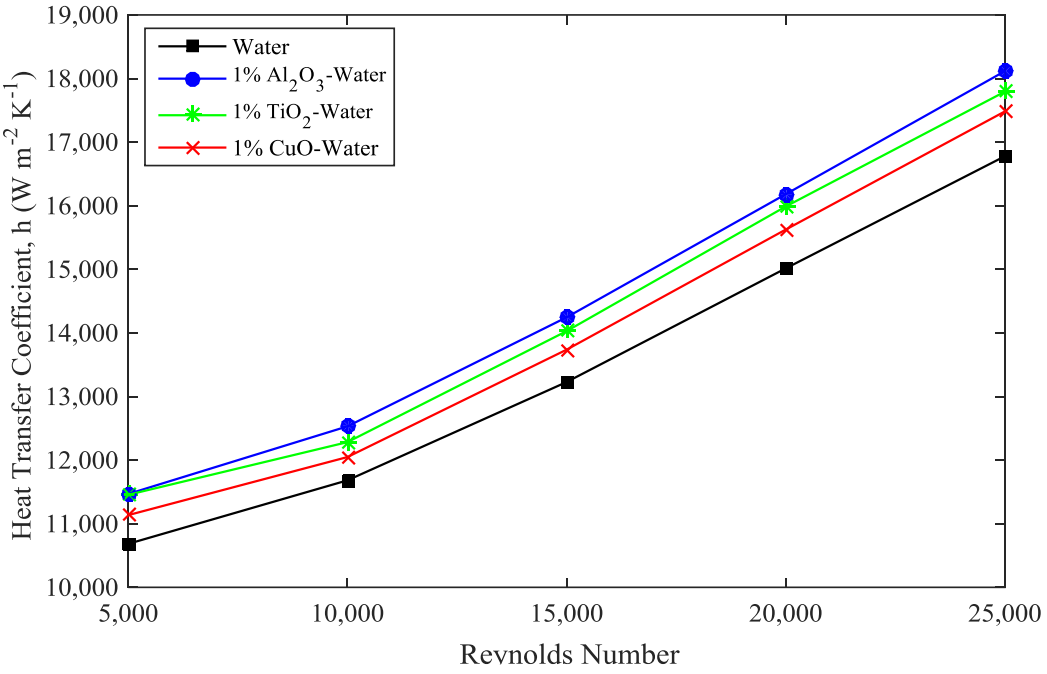

Figure 6.15 Comparison of Heat Transfer Coefficient at 1% volume fraction of nanofluids.

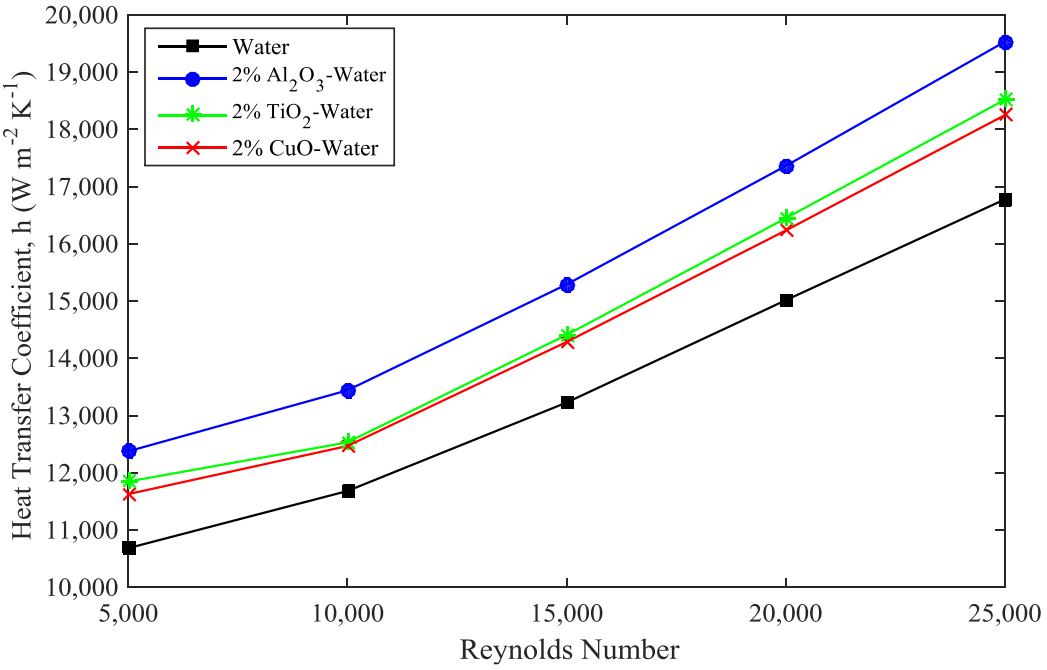

Figure 6.16 Comparison of Heat Transfer Coefficient at 2% volume fraction of nanofluids.

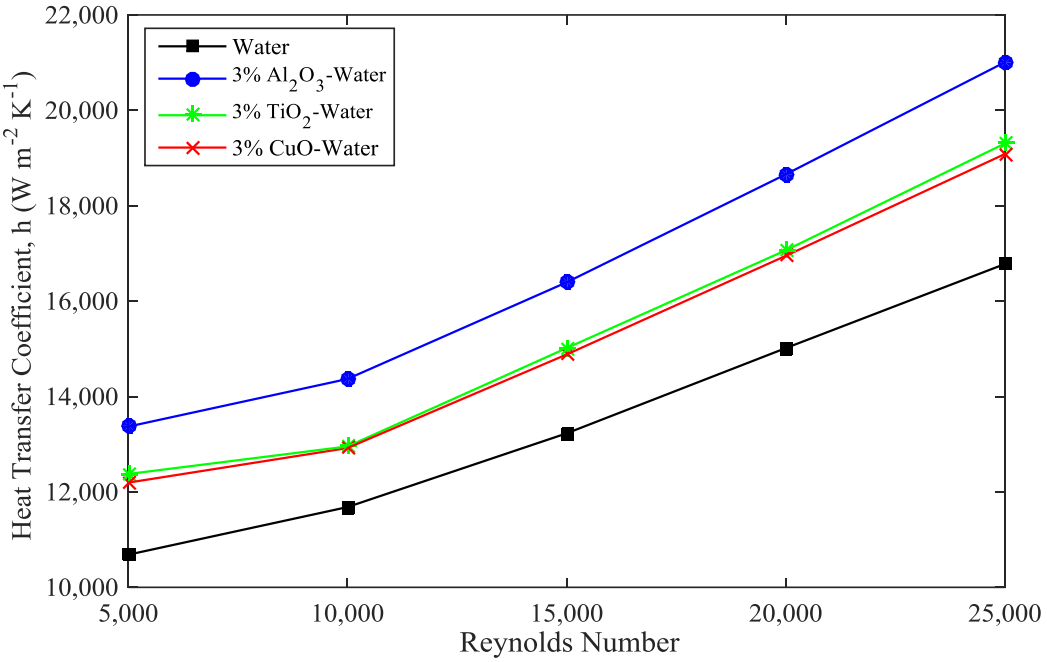

Figure 6.17 Comparison of Heat Transfer Coefficient at 3% volume fraction of nanofluids.

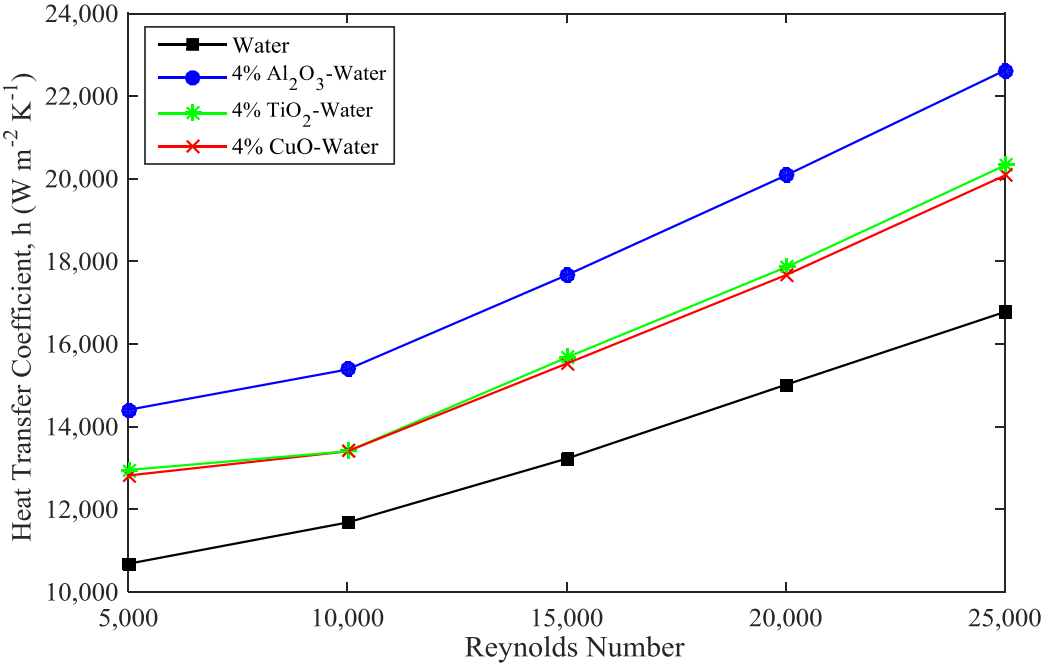

Figure 6.18 Comparison of Heat Transfer Coefficient at 4% volume fraction of nanofluids.

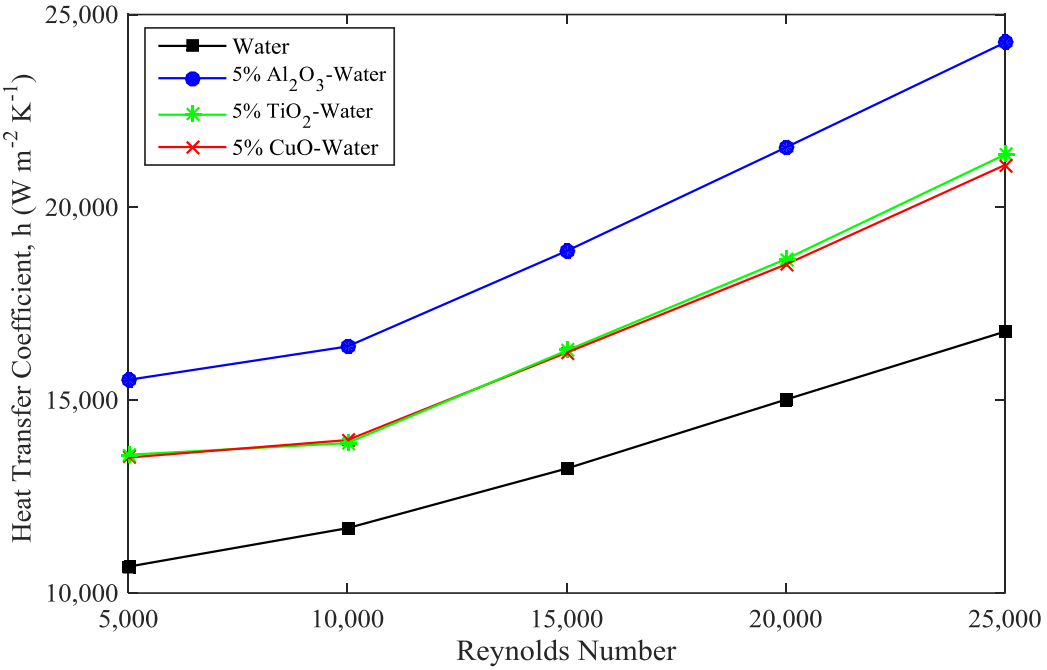

Figure 6.19 Comparison of Heat Transfer Coefficient at 5% volume fraction of nanofluids.

6.6 Pumping Power for Different Volume Fraction of Nanofluid

From figure 6.20, 6.21 and 6.22 it is evident that the requirement of pumping power increases with the increasing in Reynolds number as well as the volume fraction of the nanofluid. It is also observed that the nanofluids require more pumping power compared to pure water. At flows having a lower Reynolds number, the difference between the values of pumping power per unit length for different volume fraction is comparatively smaller.

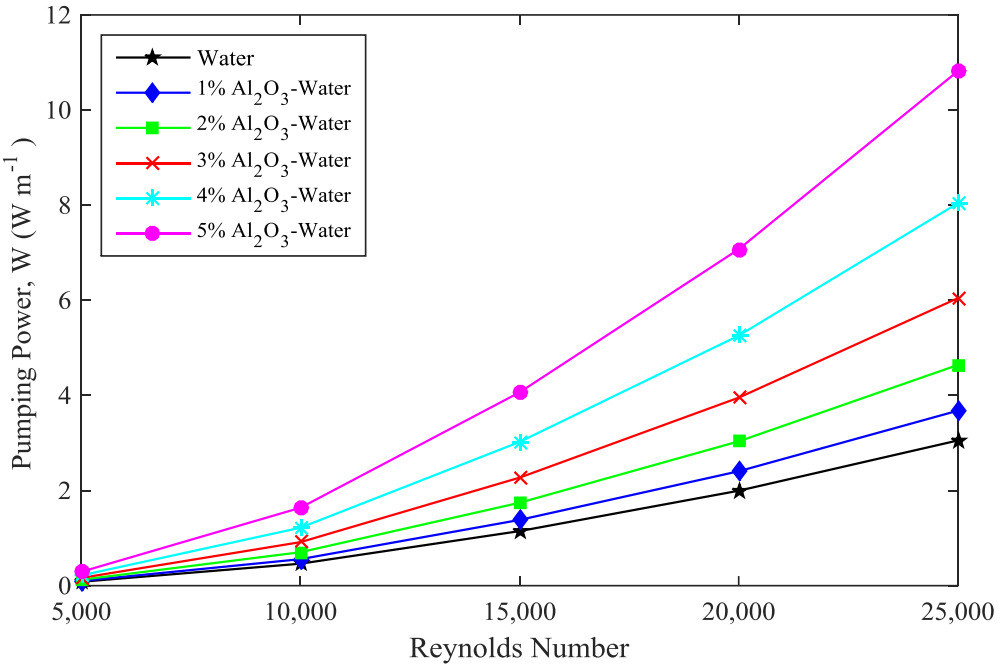

Figure 6.20 Comparison of Pumping Power for the different volume fraction of Al_2O_3-Water nanofluid.

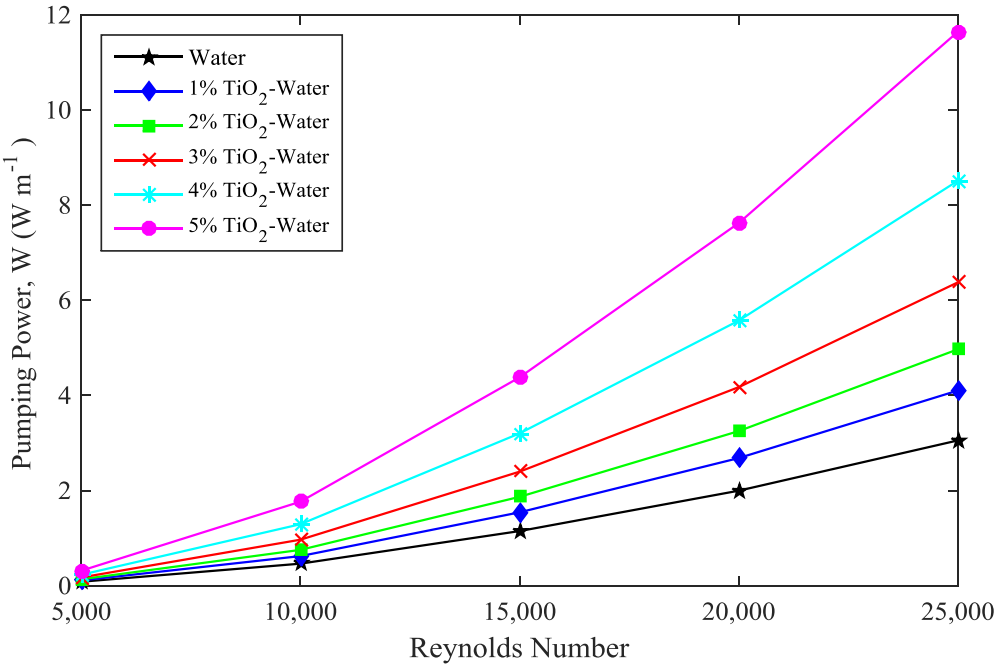

Figure 6.21 Comparison of Pumping Power for the different volume fraction of TiO_2-Water nanofluid.

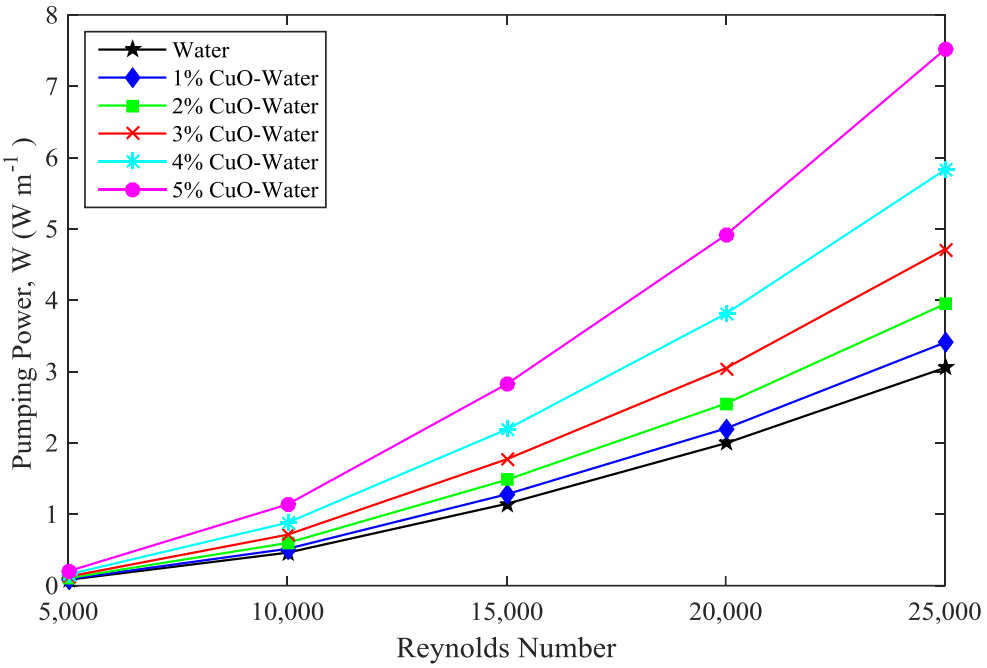

Figure 6.22 Comparison of Pumping Power for the different volume fraction of CuO-Water nanofluid.

6.7 Pumping Power at Constant Volume Fraction of Nanofluid

Figure 6.23, 6.24, 6.25, 6.26 and 6.27 indicate the variation of pumping power per unit length which are required for different nanofluids at a constant volume concentration of 1% to 5% with varying Reynolds number. From the figures, it is observed that TiO_2-water requires high pumping power than the other two nanofluids and CuO-water requires less pumping power.

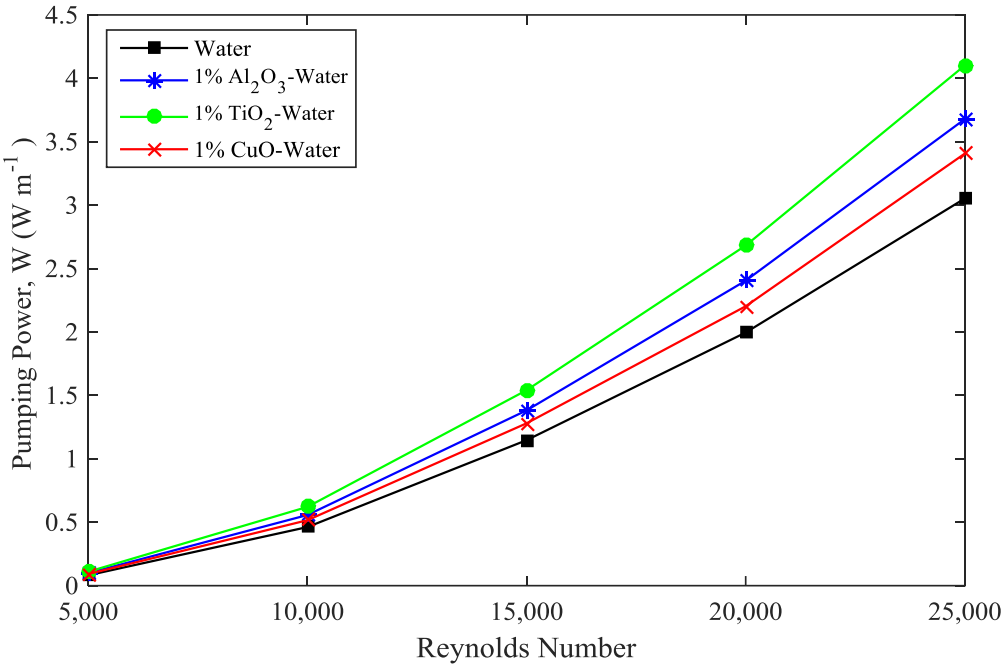

Figure 6.23 Comparison of Pumping Power at 1% volume fraction of nanofluids.

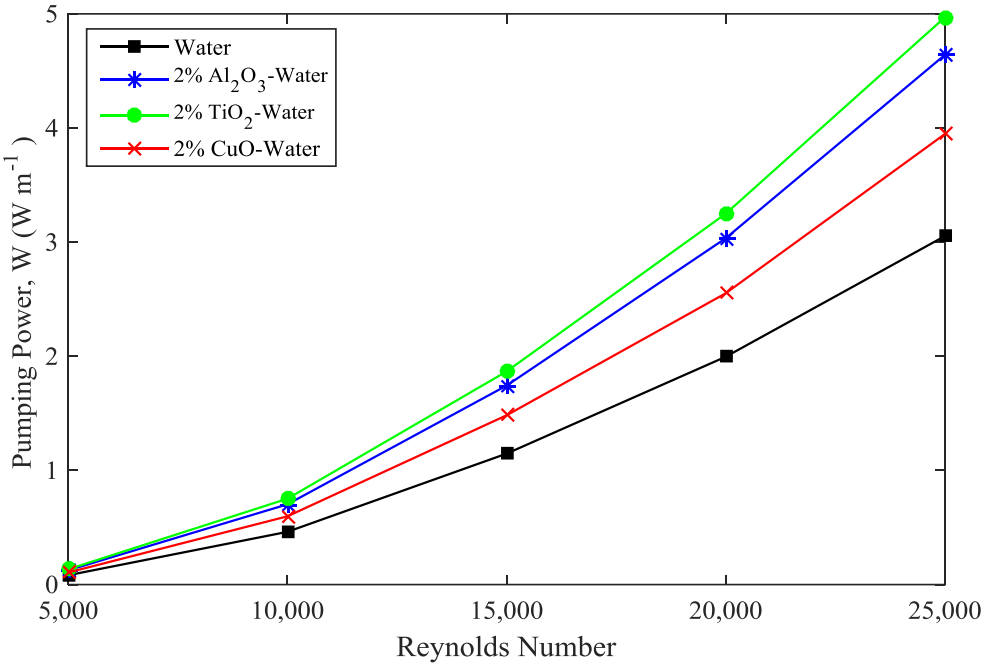

Figure 6.24 Comparison of Pumping Power at 2% volume fraction of nanofluids.

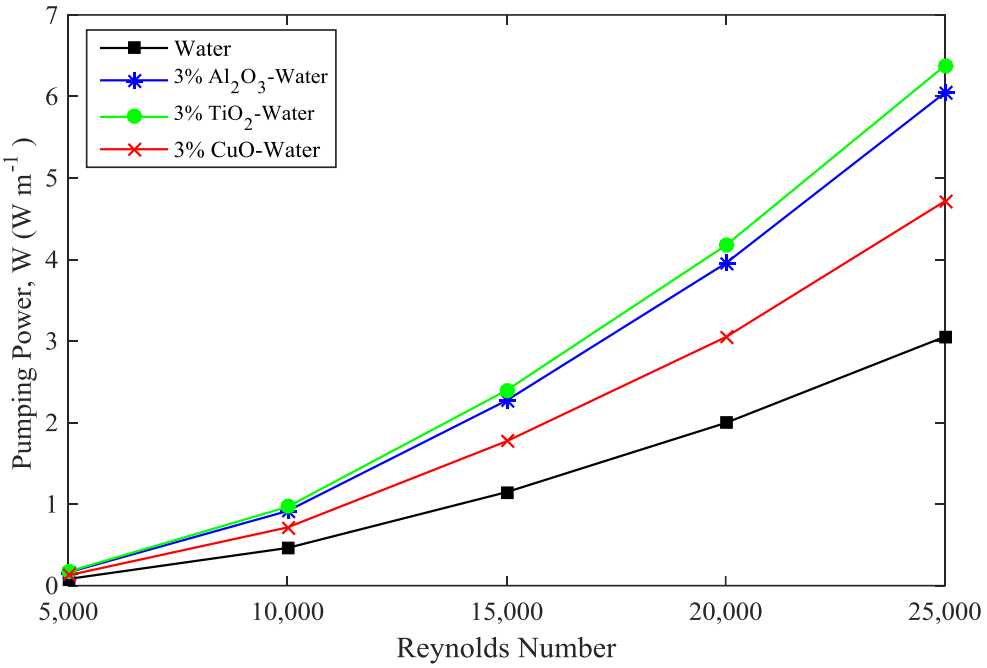

Figure 6.25 Comparison of Pumping Power at 3% volume fraction of nanofluids.

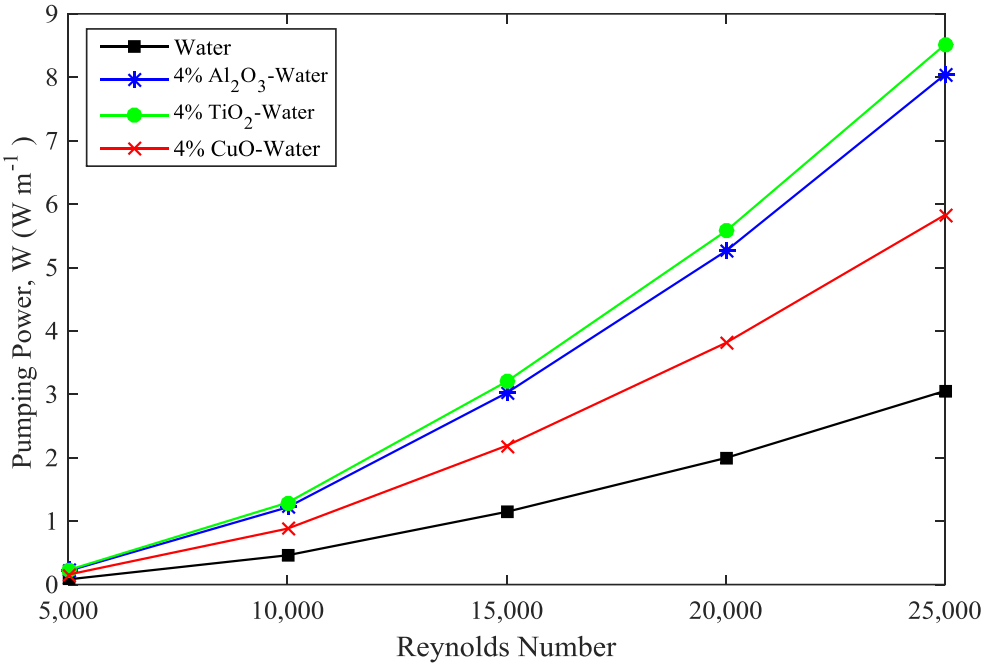

Figure 6.26 Comparison of Pumping Power at 4% volume fraction of nanofluids.

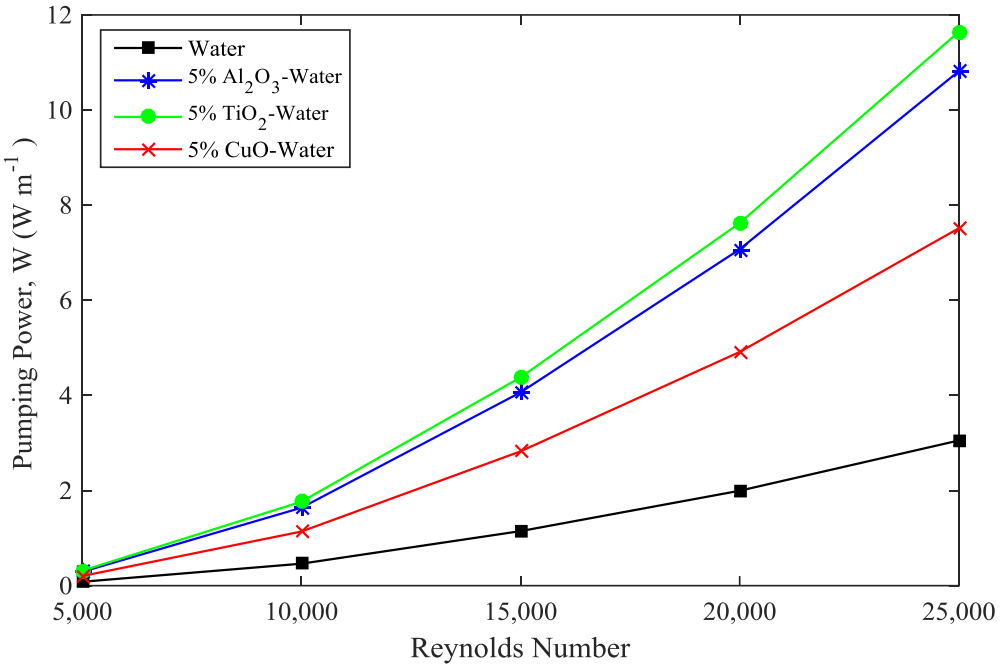

Figure 6.27 Comparison of Pumping Power at 5% volume fraction of nanofluids.

6.8 Requirement of Pumping Power Concerning to Heat Transfer Coefficient of Different Volume Fraction of the Nanofluid

Figure 6.28, 6.29 and 6.30 indicates the variation of the requirement of pumping power per unit length of the nanofluids with different values of heat transfer coefficient and volume fraction. From graphs, it has been observed that by increasing the values of heat transfer coefficient, the pumping power becomes higher. From figure 6.28 it is also observed that with the increase in the volume fraction of Al_2O_3-Water nanofluid, the requirement of pumping power decreases compared to water. At a volume fraction of 5%, the requirement of pumping power is the lowest. For TiO_2-Water nanofluid the requirement of pumping power increases with the increase in volume fraction of the nanofluid compared to water which is shown in figure 6.29. Moreover, at a volume fraction of 5%, the requirement of pumping power is the highest. For CuO-Water nanofluid the requirement of pumping power decreases with the increase of volume fraction of the nanofluid up to 2% compared to water. However, beyond 2% volume fraction, the pumping power is going to increase. Moreover, at a volume fraction of 5%, the requirement of pumping power is higher than water which is shown in figure 6.30.

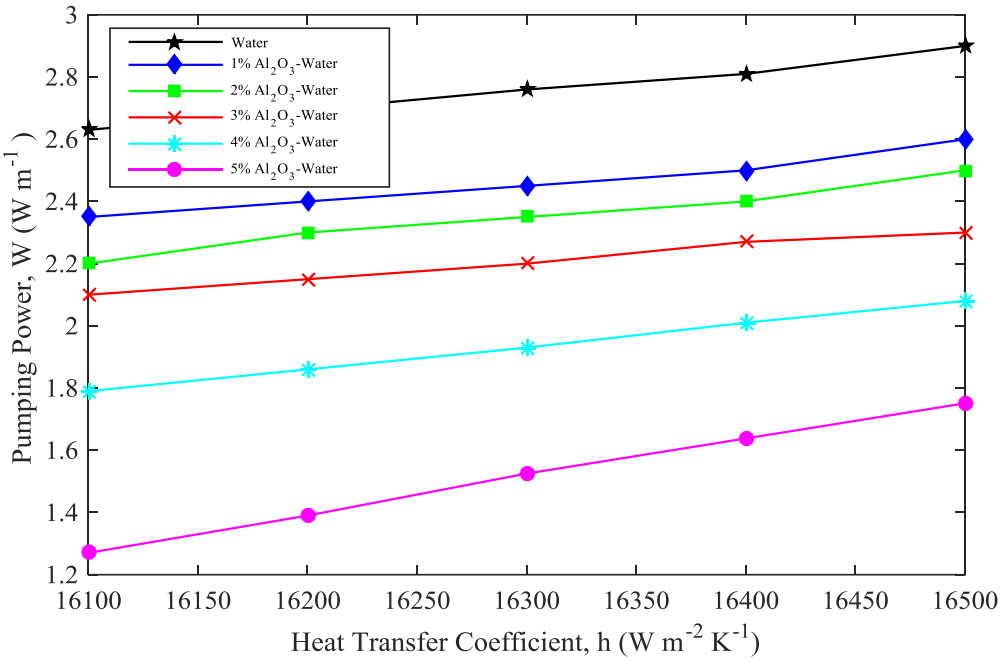

Figure 6.28 Comparison of pumping power concerning to heat transfer coefficient of the different volume fraction of Al_2O_3-Water nanofluid.

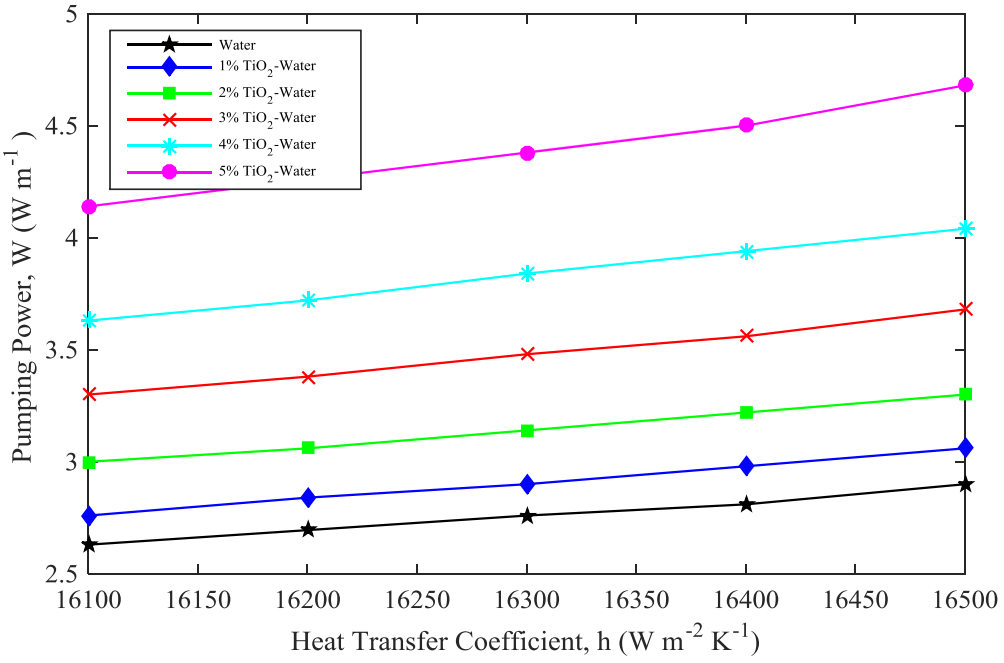

Figure 6.29 Comparison of pumping power concerning to heat transfer coefficient of the different volume fraction of TiO_2-Water nanofluid.

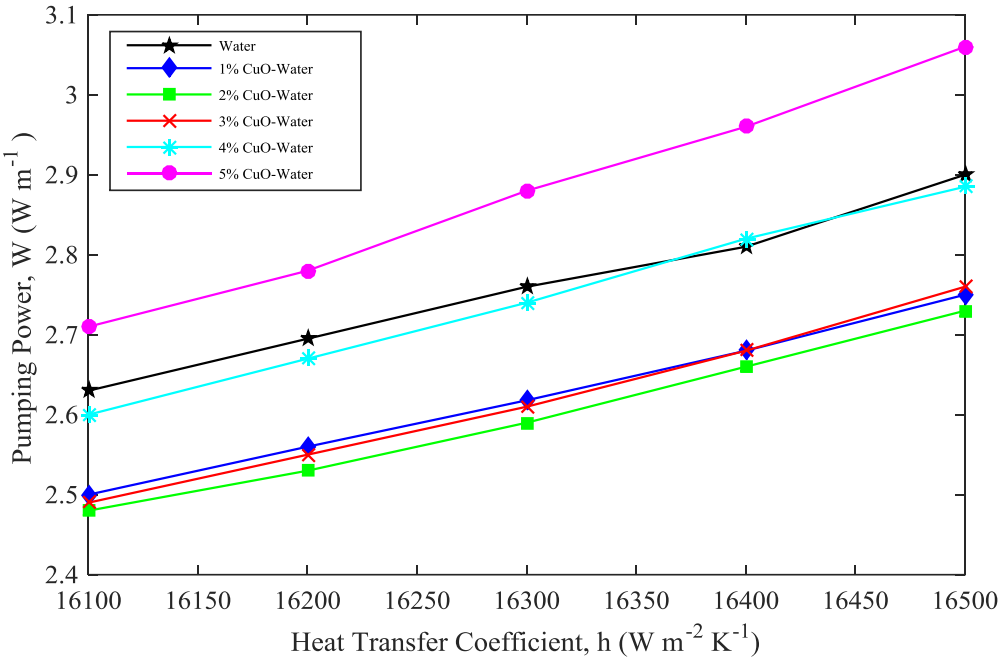

Figure 6.30 Comparison of pumping power concerning to heat transfer coefficient of the different volume fraction of CuO-Water nanofluid.

6.9 Requirement of Pumping Power Concerning to Heat Transfer Coefficient at Constant Volume Fraction of the Nanofluid

Figure 6.31, 6.32, 6.33, 6.34 and 6.35 indicate the change of pumping power with different heat transfer coefficient at a constant volume fraction. The following figures indicate that for a particular heat transfer coefficient Al_2O_3-water nanofluid requires less pumping power. On the other hand, TiO_2-water requires high pumping power than other two nanofluids compared to water.

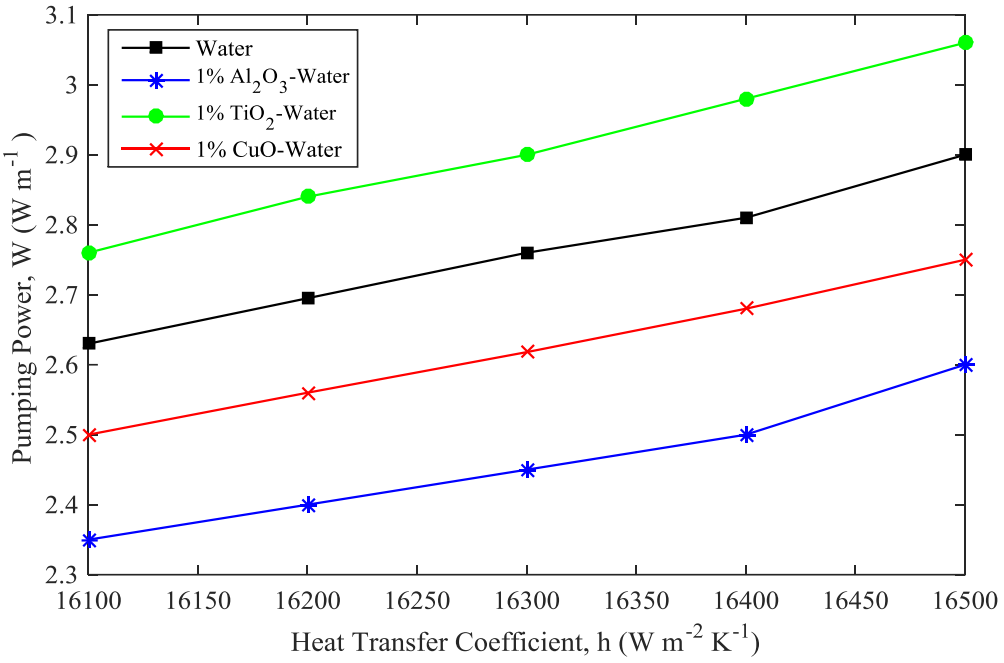

Figure 6.31 Comparison of pumping power concerning to heat transfer coefficient at 1% volume fraction of the nanofluids.

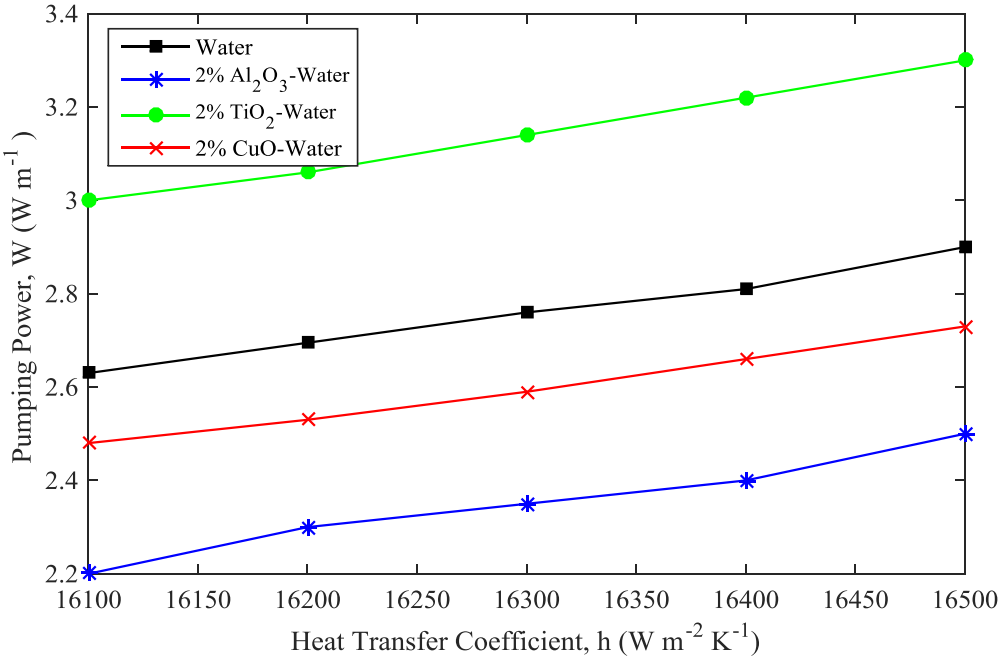

Figure 6.32 Comparison of pumping power concerning to heat transfer coefficient at 2% volume fraction of the nanofluids.

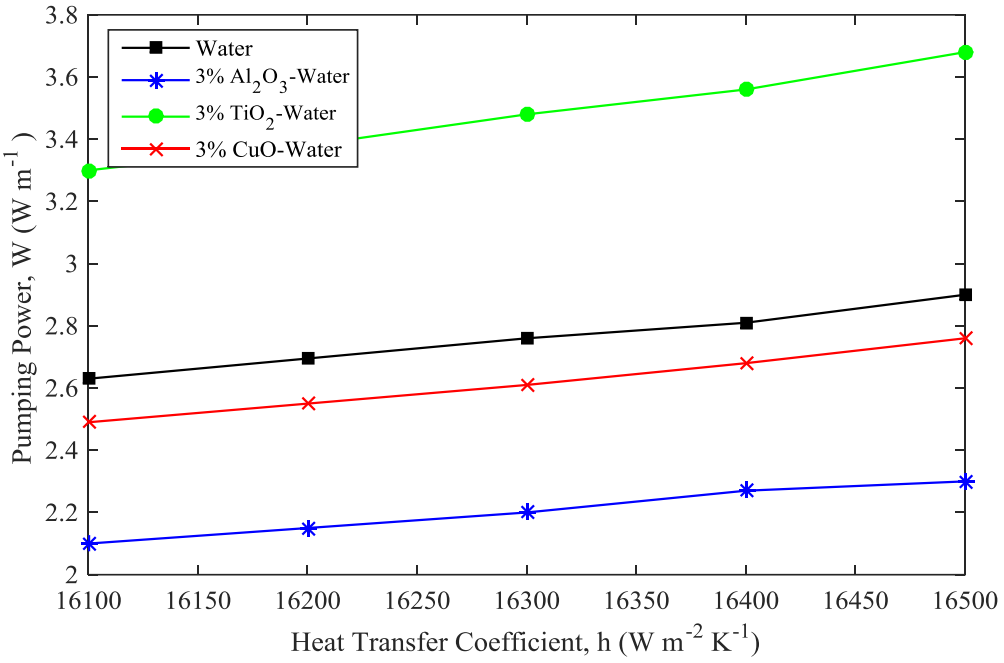

Figure 6.33 Comparison of pumping power concerning to heat transfer coefficient at 3% volume fraction of the nanofluids.

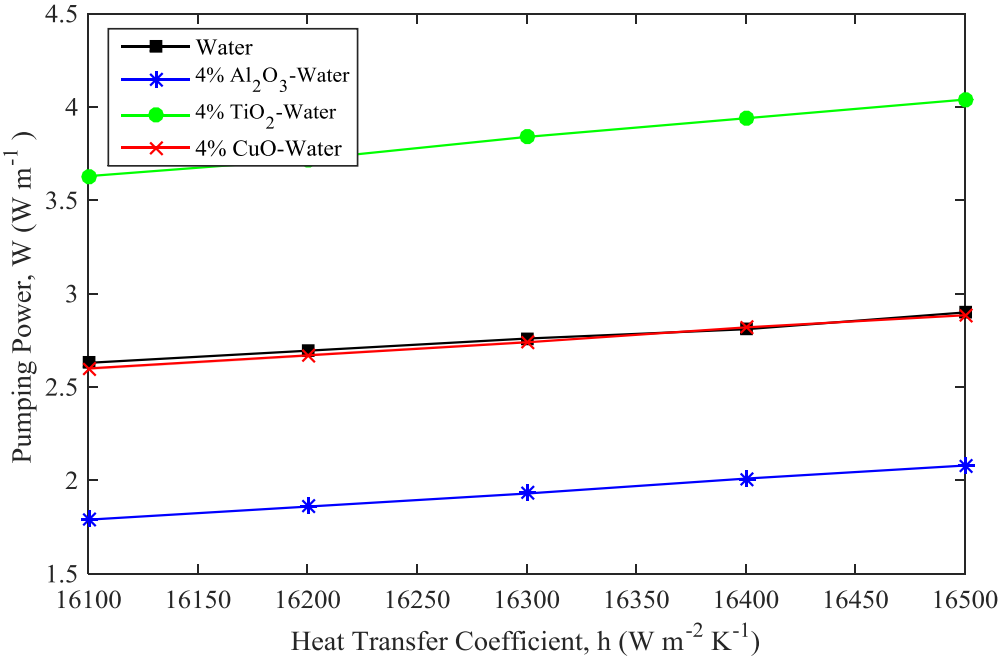

Figure 6.34 Comparison of pumping power concerning to heat transfer coefficient at 4% volume fraction of the nanofluids.

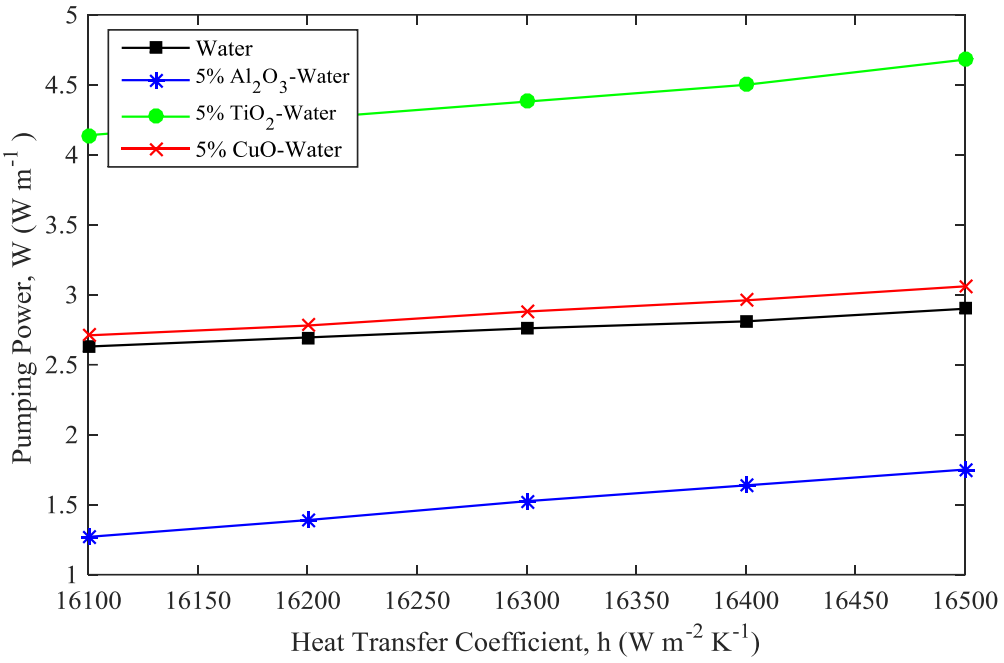

Figure 6.35 Comparison of pumping power concerning to heat transfer coefficient at 5% volume fraction of the nanofluids.

6.10 Velocity Contour, Pressure Contour, and Velocity Vector

Figure 6.36, 6.37 and 6.38 represent the contour of velocity, pressure, and the velocity vector of 5% Al_2O_3-water nanofluid.

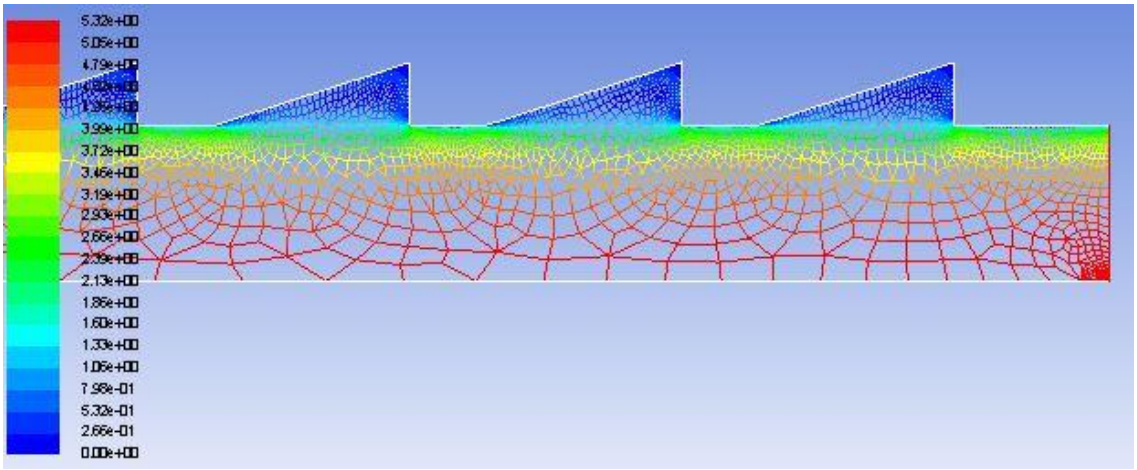

Figure 6.36 Velocity contour of Al_2O_3-water nanofluid.

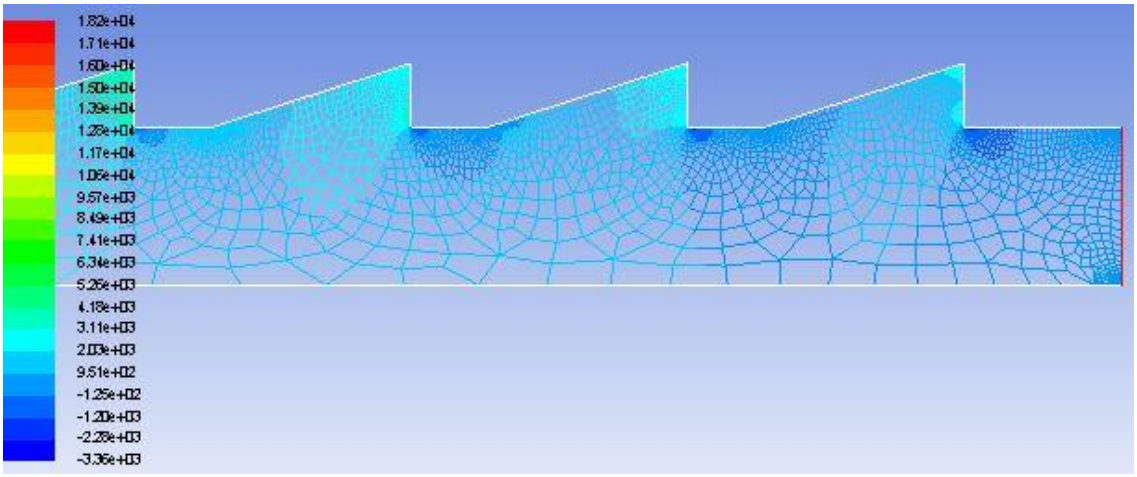

Figure 6.37 Pressure contour of Al_2O_3-water nanofluid.

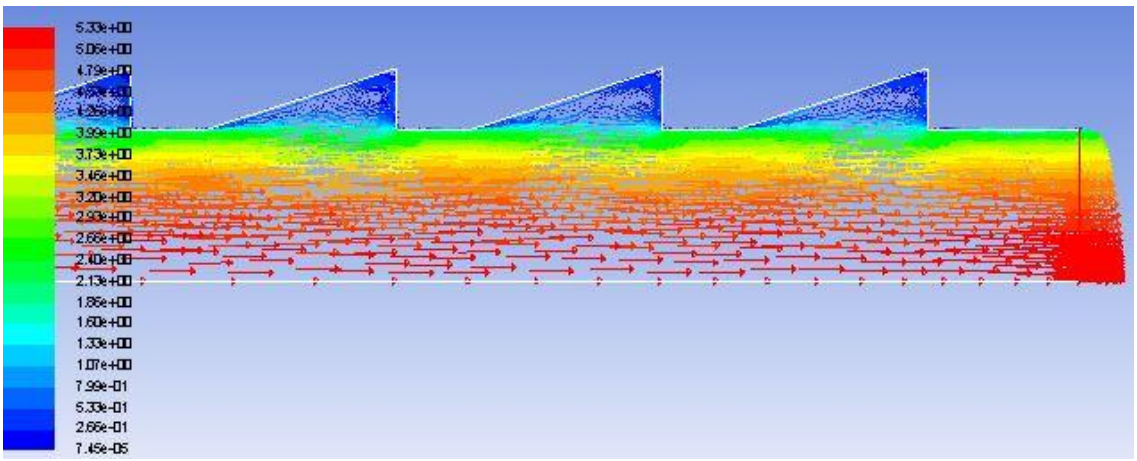

Figure 6.38 Velocity vector of Al_2O_3-water nanofluid.

Table 6.4 Comparison of the performance of the nanofluid with base fluid water (5%)

Type of fluid parameter	Water	5% Al_2O_3	5% TiO_2	5% CuO
Heat transfer coefficient ($W\ m^{-2}\ K^{-1}$)	16000	16000	16000	16000
Reynolds number	23000	8300	14400	14500
Pressure loss per unit length ($kPa\ m^{-1}$)	20.24	15.25	33.10	25.90
Viscosity ($kg\ m^{-1}\ s^{-1}$)	0.000892	0.001492	0.001531	0.001417
Density ($kg\ m^{-3}$)	996.59	1145.2605	1146.7605	1271.7605
Specific heat ($J\ kg^{-1}\ K^{-1}$)	4179.2	4008.99	4005.79	3996.49
Velocity ($m\ s^{-1}$)	2.573275	1.351614	2.403117	2.019494
Volumetric flow rate ($m^3\ s^{-1}$)	0.000129347	0.000067939	0.000120794	0.000101511
Reduction in volumetric flow rate (%)	-	47.48	6.61	21.52
Pumping power per unit length ($W\ m^{-1}$)	2.62	1.05	4.00	2.64
Power advantage ($W\ m^{-1}$)	-	1.57	-1.38	-0.02
Power advantage (%)	-	59.92	-52.67	-0.76
Mass flow rate ($kg\ s^{-1}$)	0.128906	0.077809	0.138522	0.129098
Reduction in mass flow rate (%)	-	39.64	-7.46	-0.15

Table 6.5 Comparison of the performance of the nanofluid with base fluid water (4%)

Type of fluid parameter	Water	4% Al_2O_3	4% TiO_2	4% CuO
Heat transfer coefficient ($W\ m^{-2}\ K^{-1}$)	16000	16000	16000	16000
Reynolds number	23000	11500	15600	16000
Pressure loss per unit length ($kPa\ m^{-1}$)	20.24	19.47	29.28	24.03
Viscosity ($kg\ m^{-1}\ s^{-1}$)	0.000892	0.001328	0.001355	0.001264
Density ($kg\ m^{-3}$)	996.59	1115.5264	1116.7264	1216.7264
Specific heat ($J\ kg^{-1}\ K^{-1}$)	4179.2	4043.032	4040.472	4033.032
Velocity ($m\ s^{-1}$)	2.573275	1.711299	2.366067	2.077706
Volumetric flow rate ($m^3\ s^{-1}$)	0.000129347	0.000086019	0.000118931	0.000104437
Reduction in volumetric flow rate (%)	-	33.50	8.05	19.26
Pumping power per unit length ($W\ m^{-1}$)	2.62	1.70	3.50	2.50
Power advantage ($W\ m^{-1}$)	-	0.92	-0.88	0.12
Power advantage (%)	-	35.11	-33.59	4.58
Mass flow rate ($kg\ s^{-1}$)	0.128906	0.095957	0.132814	0.127071
Reduction in mass flow rate (%)	-	25.56	-3.03	1.42

CHAPTER SEVEN

CONCLUSIONS AND RECOMMENDATIONS

7.1 Conclusions

The following conclusions are drawn to observe the effect of volume fraction of different nanofluid on heat transfer coefficient and pumping power.

a) Three different nanofluids, namely Al_2O_3-water, TiO_2-water, and CuO-water, have been analyzed through a corrugated tube to investigate the heat transfer enhancement and the pumping power advantage using finite volume based commercial CFD software ANSYS Fluent 12.

b) The heat transfer coefficient increases with the increase in volume fraction of all three nanofluids as well as with the Reynolds number.

c) These nanofluids are compared with each other, and the result indicates that the enhancement in the heat transfer coefficient is the highest for the case of Al_2O_3–water nanofluid.

d) However, CuO-water nanofluid gives a lower value of heat transfer coefficient than the other two nanofluids.

e) The value of the Nusselt number is high in case of TiO_2-water nanofluid, but the heat transfer coefficient is high in case of Al_2O_3-water nanofluid, which is occurred due to the less thermal conductivity of TiO_2-water nanofluid.

f) The value of Nusselt number, as well as heat transfer coefficient, is less increased between the Reynolds numbers of 5000 to 10000. Which is occurred because of the turbulent flow is fully developed at Reynolds number 10000.

g) Pumping power required per unit length increases with the increase in volume fraction of the nanofluid as well as Reynolds number.

h) In the case of TiO_2–water nanofluid the requirement of pumping power is higher than the other two nanofluids.

i) However CuO-water nanofluid gives lower values than the other two.

j) For a typical case study of a corrugated tube at a heat transfer coefficient 16000 W m^{-2} K^{-1} and 4% volume fraction yielded a power advantage 4.5% to 36% for CuO–water and Al_2O_3–water nanofluid whereas TiO_2–water nanofluid requires more pumping power compared to water.

7.2 Recommendations

a) The study has been done considering a particular shape of the geometry; variation in the shape of the geometry may be taken into consideration.

b) A similar study can be carried out using other nanoparticles (SiO_2, ZnO, SiC) to observe the effect on heat transfer coefficient and pumping power.

REFERENCES

[1] S.K Das, S.U.S. Choi, H.E. Patel, Heat Transfer in Nanofluids-A Review, Heat Transfer Eng. 27 (10) (2006) 3-19.

[2] S.U.S. Choi and J. A. Eastman, Enhancing thermal conductivity of fluids with nanoparticles, in The Proc. 1995 ASME Int. Mech. Eng. Congr. Expo, San Francisco, USA, ASME, FED 231/MD 66, 1995, pp. 99-105.

[3] S.U.S. Choi, Nanofluid technology: current status and future research. Korea-U.S. Technical Conference on Strategic Technologies, Vienna, VA, 1998.

[4] S.U.S. Choi, Z.G. Zhang, W. Yu, F.E. Lockwood, E.A. Grulke, Anomalous thermal Conductivity enhancement in nanotube suspensions. Appl. Phys. Lett., 79(14) (2001), 2252-2254.

[5] Y. Xuan, Q. Li, Heat transfer enhancement of nanofluids, International Journal of heat and Fluid flow 21 (2000) 58-64.

[6] Laurent Piccolo, Ana Valcarcel, Marta Bausach, Cécile Thomazeau, Denis Uzio, and Gilles Berhault, "Tuning the shape of nanoparticles to control their catalytic properties: selective hydrogenation of 1,3 – butadiene on Pd/Al_2O_3", Physical chemistry chemical physic, 2008.

[7] John Philip, P.D. Shima: Thermal properties of nanofluids: Advances in Colloid and Interface Science, volumes 183-184, 15 November 2012, Pages 30-45.

[8] Linghui Kong, Jianlin Sun and Yueyue Bao, "Preparation, characterization and tribological mechanism of nanofluids," Royal Society Chemistry, RSC Adv., 2017, 7, 12599-12609.

[9] Sayantan Mukherjee, Somjit Paria, "Preparation and Stability of Nanofluids"–A Review. IOSR Journal of Mechanical and Civil Engineering, e-ISSN: 2320-334X, Volume 9, Issue 2 (Sep.-Oct. 2013), PP 63-69.

[10] P Keblinski, J A Eastman, D G Cahill, "Nanofluids for thermal transport" Materials Today Volume 8, Issue 6, June 2005, Pages 36-44.

[11] Kim, J. K., Jung, J. Y., & Kang, Y. T. (2007). Absorption performance enhancement by nanoparticles and chemical surfactants in a binary nanofluid. International Journal of Refrigeration, 30(1), 50-57.

[12] Demirbas MF. Thermal energy storage and phase change materials: an overview. Energy Sources, Part B: Economics, Planning, and Policy. 2006; 1(1):85–95.

[13] K.G. Kalpana Sarojini, Siva V.Manoj, Pawan K. Singh, T. Pradeep, Sarit K. Das: Colloids and Surfaces: A-physicochemical and Engineering Aspects: 417(2013) 39-46.

[14] Pramod Warrier and Amyn Teja, "Effect of particle size on the thermal conductivity of nanofluids containing metallic nanoparticles," 2011 Mar 22.

[15] P.Vassallo, R. Kumar, and S.D. Amico. Pool boiling heat transfer experiments in silica-water nanofluids, International Journal of Heat and Mass Transfer 47, 2004, 407-411.

[16] T. Sharma, A. L. M. Reddy, T. S. Chandra, and S. Ramaprabhu, "Development of carbon nanotubes and nanofluids based microbial fuel cell," International Journal of Hydrogen Energy, vol. 33, no. 22, pp. 6749–6754, 2008.

[17] Behzadmehr A, Saffar-Avval M, Galanis N. Prediction of turbulent forced convection of a nanofluid in a tube with uniform heat flux using a two-phase approach.Int J Heat Fluid Flow 2007;28(2):211-19.

[18] Santra AK, Sen S, Chakraborty N. Study of heat transfer due to laminar flow of copper-water nanofluid through two isothermally heated parallel plates. Int J Therm Sci 2009; 48 (2):391-400.

[19] Heidary H, Kermani MJ. Effect of nano-particles on forced convection in the sinusoidal-wall channel. Int Commun Heat Mass Transf 2010; 37(10):1520-7.

[20] Ahmed MA, Shuaib NH, Yusoff MZ, Al-Falahi AH. Numerical investigations of flow and heat transfer enhancement in a corrugated channel using nanofluid. Int Commun Heat Mass Transf 2011; 38(10):1368-75.

[21] Vatani A, Mohammed HA. Turbulent nanofluid flow over periodic rib-grooved channels. Eng Appl Comput Fluid Mech 2013; 7(3):369-81.

[22] Talebi F, Mahmoudi AH, Shahi M. Numerical study of mixed convection flows in a square lid-driven cavity utilizing nanofluid. Int Commun Heat Mass Transf 2010; 37(1):79-90.

[23] Abu-Nada E, Masoud Z, Hijazi A. Natural convection heat transfer enhancement in horizontal concentric annuli using nanofluids. Int Commun Heat Mass Transf 2008; 35(5):657-65.

[24] Akbarinia A, Behzadmehr A. Numerical study of laminar mixed convection of a nanofluid in horizontal curved tubes. Appl Therm Eng 2007; 27(8):1327-37.

[25] Hussein AM, Sharma KV, Bakar RA, Kadirgama K. The effect of cross-sectional area of the tube on friction factor and heat transfer nanofluid turbulent flow. Int Commun Heat Mass Transf 2013; 47:49-55.

[26] Peyghambarzadeh SM, Hashemabadi SH, Seifi Jamnani M, Hoseini SM. Improving the cooling performance of automobile radiator with Al2O3-water nanofluid. Appl Therm Eng 2011; 31(10):1833-8.

[27] Ijam A, Saidur R. Nanofluid as a coolant for electronic devices (cooling of electronic devices). Appl Therm Eng 2012; 32:76-82.

[28] Clancy EV. Apparatus and method of using nanofluids to improve the energy efficiency of vapor compression systems. U.S. Patent Application 12/841,089, filed July 21, 2010.

[29] Firouzfar E, Soltanieh M, Noie SH, Saidi MH. Investigation of heat pipe heat exchanger effectiveness and energy saving in air conditioning systems using silver nanofluid. Int J Environ Sci Technol 2012; 9(4):587-94.

[30] Maghrebi MJ, Nazari M, Armaghani T. Forced convection heat transfer of nanofluids in a porous channel. Transp Porous Media 2012; 93(3):401-13.

[31] Harikrishnan S, Kalaiselvam S. Experimental investigation of solidification and melting characteristics of nanofluid as PCM for solar water heating systems. In: International conference on energy resources & technologies for sustainable development, Department of Mechanical Engineering Bengal Engineering and Science University, Shibpur, Howrah, vol. 711103.

[32] Duangthongsuk W, Wongwises S. Heat transfer enhancement and pressure drop characteristics of TiO2-water nanofluid in a double-tube counter flow heat exchanger. Int J Heat Mass Transf 2009; 52(7):2059-67.

[33] Farajollahi B, Etemad S Gh, Hojjat M. Heat transfer of nanofluids in a shell and tube heat exchanger. Int J Heat Mass Transf 2010; 53(1):12-17.

[34] Fard MH, Talaie MR, Nasr S. Numerical and experimental investigation of heat transfer of Zno/Water nanofluid in the concentric tube and plate heat exchangers. Therm Sci 2011; 15(1).

[35] Leong KY, Saidur R, Mahlia TMI, Yau YH. Modeling of the shell and tube heat recovery exchanger operated with nanofluid based coolants. Int J Heat Mass Transf 2012; 55(4):808-16.

[36] Gunnasegaran P, Shuaib NH, Abdul Jalal MF, Sandhita E. Numerical study of fluid dynamic and heat transfer in a compact heat exchanger using nanofluids. ISRN Mechanical Engineering 2012; 2012.

[37] Zamzamian A, Oskouie SN, Doosthoseini A, Joneidi A, Pazouki M. Experimental investigation of forced convective heat transfer coefficient in nanofluids of Al2O3/EG and CuO/EG in a double pipe and plate heat exchangers under turbulent flow. Exp Therm Fluid Sci 2011; 35(3):495-502.

[38] Kannadasan N, Ramanathan K, Suresh S. Comparison of heat transfer and pressure drop in horizontal and vertical helically coiled heat exchanger with CuO/water based nanofluids. Exp Therm Fluid Sci 2012; 42:64-70.

[39] Pantzali MN, Kanaris AG, Antoniadis KD, Mouza AA, Paras SV. Effect of nanofluids on the performance of a miniature plate heat exchanger with the modulated surface. Int J Heat Fluid Flow 2009; 30(4):691-9.

[40] Pandey SD, Nema VK. Experimental analysis of heat transfer and friction factor of nanofluid as a coolant in a corrugated plate heat exchanger. Exp Therm Fluid Sci 2012; 38:248-56.

[41] Elias MM, Miqdad M, Mahbubul IM, Saidur R, Kamalisarvestani M, Sohel MR, et al. Effect of nanoparticle shape on the heat transfer and thermodynamic performance of a shell and tube heat exchanger. Int Commun Heat Mass Transf 2013; 44:93-9.

[42] Sonawane SS, Khedkar RS, Wasewar KL. Study on concentric tube heat exchanger heat transfer performance using Al2O3water based nanofluids. Int Commun Heat Mass Transf 2013; 49:60-8.

[43] M.N. Pantzali, A.A. Mouza, S.V. Paras: Investigating the efficacy of nanofluids as coolants in plate heat exchangers (PHE): Chemical Engineering Science 64 (2009) 3290-3300.

[44] Hai-tao Zhu, Yu-sheng Lin, Yan-sheng Yin: A novel one-step chemical method for preparation of copper nanofluids: Journal of Colloid and Interface Science 277 (2004) 100-103.

[45] Dongsheng Wen, Guiping Lin, SaeidVafaei, Kai Zhang: Review of nanofluids for heat transfer applications: Particuology 7 (2009) 141-150.

[46] Nader Nikkam, Morteza Ghanbarpour, Mohsin Saleemi, Ehsan Bitaraf Haghighi: Experimental investigation on thermo-physical properties of copper/diethylene glycol nanofluids fabricated via microwave-assisted route: Applied Thermal Engineering Volume 65, Issues 1–2, April 2014, Pages 158-165.

[47] Lin Lu, Lun-Chun Lv, Zhen-Hua Liu: Application of Cu- water and Cu- ethanol nanofluids in a small flat capillary pumped loop: Thermochimica Acta 512 (2011) 98-104.

[48] Duangthongsuk W, Wongwises S. Heat transfer enhancement and pressure drop characteristics of TiO_2-water nanofluid in a double-tube counter flow heat exchanger. Int J Heat Mass Transf 2009; 52(7):205967.

[49] Williams, W., Buongiorno, J., and Hu, L.-W., 2008, "Experimental Investigation of Turbulent Convective Heat Transfer and Pressure Loss of Alumina/Water and Zirconia/Water Nanoparticle Colloids (Nanofluids) in Horizontal Tubes," ASME J. Heat Transfer, 130(4), p. 042412.

[50] Rea, U., McKrell, T., Hu, L.-W., and Buongiorno, J., 2009, "Laminar Convective Heat Transfer and Viscous Pressure Loss of Alumina-Water and Zirconia-Water Nanofluids," Int. J. Heat Mass Transfer, 52, pp. 2042–2048.

[51] Heris, S.Z.; Nassan, T.H.; Noie, S.H.; Sardarabadi, H.; Sardarabadi, M. Laminar convective heat transfer of Al2O3/water nanofluid through the square cross-sectional duct. Int. J. Heat Fluid Flow 2013, 44, 375–382.

[52] Akbarzadeh, M.; Rashidi, S.; Bovand, M.; Ellahi, R. A sensitivity analysis on thermal and pumping Power for the flow of nanofluid inside a wavy channel. Journal of Molecular Liquids Volume 220, August 2016, Pages 1-13.

[53] M.H. Kayhani, H. Soltanzadeh, M.M. Heyhat, M. Nazari, F. Kowsary, Experimental study of Convective heat transfer and pressure drop of TiO_2-water nanofluid, International Communication in Heat and Mass Transfer 39 (2012) 456– 462.

[54] K. Abdul Hamid, W.H. Azmi, RizalmanMamat, K.V. Sharma, Experimental investigation on heat transfer performance of TiO_2 nanofluids in water–ethylene glycol mixture, International Communications in Heat and Mass Transfer 73 (2016) 16–24.

[55] B. C. Pak, and Y. I. Cho. "Hydrodynamic and heat transfer study of dispersed fluids with submicron metallic oxide particles," Exp. heat transfer, vol.11, 1998, pp.151-170.

[56] E.B. Maiga, C.T.Nguyen, N. Galanis and G. Roy, “Heat transfer behaviors of nanofluids in a uniformly heated tube,” Superlattices and Microstructures, vol.35, pp. 2004, pp.543 –557.

[57] Corcione M. Heat transfer features of buoyancy-driven nanofluids inside rectangular enclosures differentially heated at the sidewalls. Int J Therm Sci 2010; 49 (9):1536-46.

[58] Maxwell, J.C., Treatise on Electricity and Magnetism. Clarendon Press, Oxford, UK, second edition.

[59] Y. Xuan, W. Roetzel, Conceptions for heat transfer correlation of nanofluids, Int. J. Heat Mass Transfer 43 (2000) 3701–3707.

[60] Notter RH, Sleicher CA. A solution to the turbulent Graetz problem—III Fully developed and entry region heat transfer rates. Chem Eng Sci 1972; 27 (11):2073-93.